



Original Article

A review on stamp forming of continuous fibre-reinforced thermoplastics



Richard A. Brooks ^a, Hongyan Wang ^b, Zerong Ding ^b, Jie Xu ^c, Qinghua Song ^c,
 Haibao Liu ^a, John P. Dear ^a, Nan Li ^{b,*}

^a Department of Mechanical Engineering, Imperial College London, London, SW7 2AZ, UK

^b Dyson School of Design Engineering, Imperial College London, London, SW7 2AZ, UK

^c Commercial Aircraft Corporation of China, Ltd. COMAC, 1919 Shibo Avenue, Pudong District, Shanghai, China

ARTICLE INFO

Article history:

Received 28 March 2022

Accepted 4 May 2022

Available online 10 May 2022

Keywords:

Continuous fibre-reinforced thermoplastics

Stamp forming

Deformation mechanisms

Defects

Process parameters

ABSTRACT

Continuous fibre-reinforced thermoplastics (FRTPs) are replacing metals in certain applications in the aerospace industry due to their superior properties e.g., high strength-to-weight ratio and good fatigue resistance. Adopting these lightweight materials in vehicles is a solution for improving vehicle efficiency across the transport industry. Among various manufacturing techniques for FRTP parts, stamp forming is one of the most advantageous when small structures and mass production are targeted. However, a significant barrier for this technique is the quality control of manufacturing. The current paper reviews the development of stamp forming technology, benefits of using such technology and the typical quality issues in stamp forming of FRTP parts. First, advantages of stamp forming, compared to other thermoforming techniques, are discussed, followed by a review of the historical development of the process. Second, deformation mechanisms of FRTPs during stamp forming are examined, with particular focuses on the frictional behaviour and testing thereof. Third, the main defects associated with stamp forming are considered, alongside suggestions towards reducing their presence. Finally, an extensive survey of the effect of process parameters on the mechanical properties of formed parts is included, with generally expected trends highlighted and methodologies for finding optimum conditions presented. Based on the thorough review of state-of-the-art stamp forming, future trends and research gaps to be tackled for widening the applicability of FRTP stamp forming are suggested.

© 2022 The Authors. Publishing services by Elsevier B.V. on behalf of KeAi Communications Co. Ltd. This is an open access article under the CC BY-NC-ND license (<http://creativecommons.org/licenses/by/4.0/>).

1. Introduction

The aerospace and automotive industries are significant contributors to worldwide greenhouse gas emissions [1,2] and the issue of climate change has led to a drive towards improving energy efficiency and reducing emissions. In the aerospace industry, the cost savings associated with improved fuel efficiency act as an incentive for this development. In the automotive industry, regulations establishing limits on the emissions produced by new vehicles help ensure targets are reached [2]. A significant contributor to this reduction in emissions is the development and application of lightweight materials which give the required strength for structural

integrity and safety. Fibre-reinforced polymers (FRPs) are known for their high strength-to-weight ratio and are now widely used in aerospace structures and increasingly used in the automotive industry. For example, composites comprise 53% [3] and 50% [4] of the total structural weight of the Airbus A350-900 XWB and Boeing 787 Dreamliner, respectively. The Boeing 787 is therefore 20% lighter than other aircraft of a similar configuration, leading to a 10–12% improvement in fuel efficiency [5]. As an important type of composite materials, fibre-reinforced thermoplastics (FRTPs) which have excellent formability and recyclability, are also finding more and more applications. This review focuses on continuous FRTPs due to their superior mechanical properties compared to short or discontinuous fibre-reinforced polymers [6]. In this introduction, the structure of continuous FRTPs is discussed, followed by an analysis of the advantages of the stamp forming process compared to other thermoforming methods. A summary of the development of the stamp forming process is also included.

* Corresponding author.

E-mail address: n.li09@imperial.ac.uk (N. Li).

Peer review under responsibility of Editorial Board of International Journal of Lightweight Materials and Manufacture.

1.1. Continuous FRTPs

Continuous FRTPs are formed of multiple plies of FRTP pre-preg. Each ply is formed of high modulus fibres, often made from carbon or glass, within a thermoplastic (TP) matrix, such as poly(ether ether ketone) (PEEK) or poly(phenylene sulphide) (PPS). The fibres, also known as the reinforcement, provide much of the strength and stiffness whereas the matrix holds the fibres together and transfers the load as well as contributing to the toughness [8]. The fibres can either all be aligned in the same direction (unidirectional (UD)), see macro-scale schematic in Fig. 1(a), or woven together to form a fabric, see macro-scale schematic in Fig. 1(b). Note that the UD schematic shows two plies whereas the woven schematic only depicts one. The meso- and micro-scale schematics in Fig. 1 demonstrate the fibre structure when viewed at shorter length scales. When laid on top of each other and consolidated into a single sheet, these plies (both UD and woven) form a laminate. An alternative to pre-preg is commingled fabric, in which carbon or glass fibres are mingled into bundles along with fibres made of polymer. Commingled fabrics can be designed to be highly drapable and thus suitable for forming. When heat is applied the thermoplastic yarn melts and, after pressure application and cooling, a rigid composite is formed [9]. Thermoset matrix FRPs are widely used in aerospace but thermoplastic matrix FRPs, a.k.a. FRTPs, have replaced thermoset matrix FRPs in some applications. In contrast to their thermosetting counterparts, FRTPs can melt and therefore be formed under high temperatures, without needing to undergo a time-consuming cure cycle. This gives potential regarding large-scale, fast and economical production processes and has led to increased interest in FRTPs as an alternative to commonly used thermoset matrix composites. Further advantages of TP matrices include improved impact resistance [10] and the potential for recycling or remoulding [11].

1.2. Stamp forming versus other thermoforming methods for FRTPs

The most common forming method for FRTPs involves pre-preg (material containing fibres pre-impregnated with resin) being placed into a mould by hand and then processed in an autoclave.

This conventional method of lay-up followed by autoclave processing is time-consuming, energy-intensive and expensive [12,13] so is not appropriate for high volume production. Other thermoforming methods which do not require hand lay-up are detailed below.

Stamp forming allows relatively complex shapes to be formed comparatively quickly from pre-consolidated composite laminates. A general stamp forming process using a matched metal die set is shown in Fig. 2. Stamp forming involves heating a material (usually to above the matrix melting temperature, T_m , in the case of FRTPs) (Fig. 2(a)) before transferring the material to a matched metal die or mould set (Fig. 2(b)). The two halves of the mould are brought together and the heated material is deformed into the shape of the mould (Fig. 2(c)). After a given holding time, the mould sections move apart and the formed part is removed (Fig. 2(d)).

In rubber forming, the laminate is formed between a pair of dies made from different materials. One is rigid (usually made of metal, as in the stamp forming process) and the other is made of rubber [14]. The laminate is heated to above T_m , transferred to the tool and pressed into shape when the dies close. This process can be considered similar to the stamp forming process, but with one die made from rubber instead of metal.

In double-diaphragm forming, flexible diaphragms surround the laminate on each side and are clamped on top of a mould [14]. A similar single-diaphragm forming process uses only one diaphragm; however, this makes forming double curvature shapes difficult [15]. The diaphragm forming assembly is usually placed into an autoclave, the area between the diaphragms is put under vacuum and the material is heated to above T_m [16]. Air pressure is applied to one side which forces the diaphragms and laminate into the shape of the mould. The laminate can slide between the diaphragms and the subsequent interfacial shear stresses create tensile stresses within the laminate [17]. This means out-of-plane wrinkling is restricted due to the presence of the diaphragms [18]. Therefore, high quality parts can be produced.

Hydroforming is similar to double-diaphragm forming in that a fluid is used to deform a diaphragm. However, in this method, a pressurised hydraulic fluid, rather than pressurised air, behind a rubber diaphragm is used to form the laminate against a mould

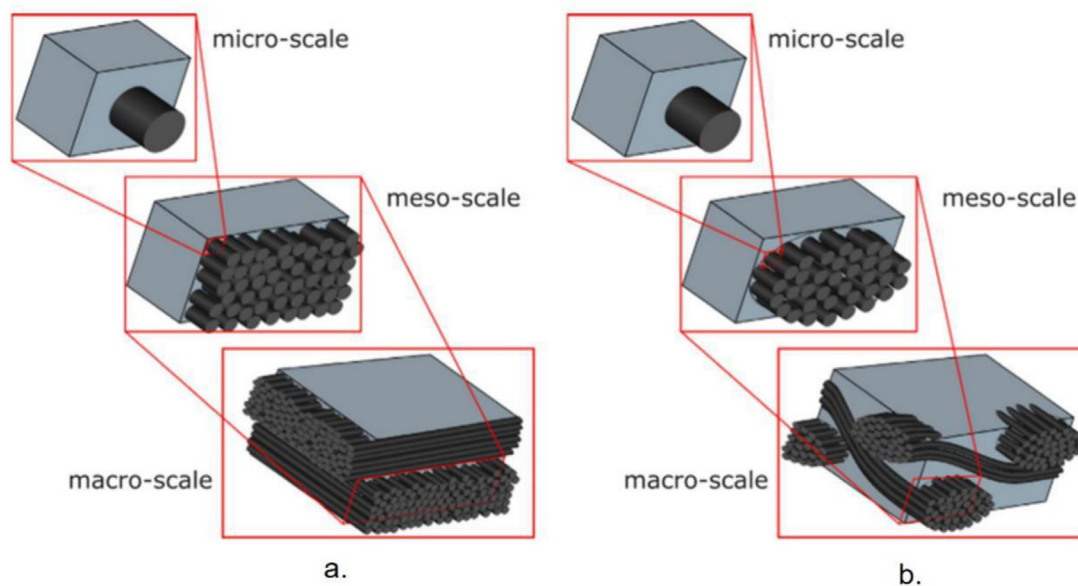


Fig. 1. Multi-scale structures of (a) unidirectional (UD) and (b) woven composite [7].

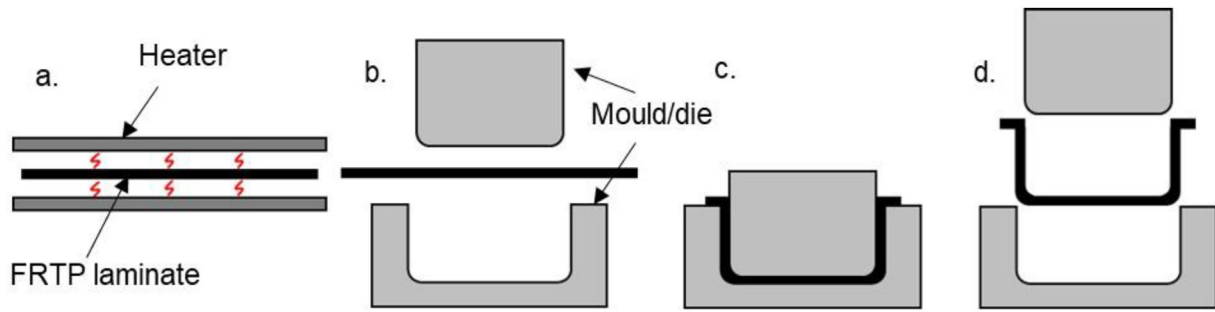


Fig. 2. Typical stamp forming process for FRTPs, showing stages: (a) heating, (b) transfer, (c) forming, (d) removal.

[17]. These systems have been known to generate pressures of up to 10,000 psi and have been widely utilised in the sheet metal forming industry.

Although the rubber die used in rubber forming can give a more even pressure distribution across the part compared to the metal die used in stamp forming, complex details are difficult to produce and there are limitations on the forming temperature which can be used to allow a suitable working life for the die [15,17]. In addition, the low thermal diffusivity of the rubber die leads to reduced cooling rates and increased cycle times, making this method less suitable for large volume manufacturing [15]. While diaphragm forming can restrict wrinkle formation and give high quality parts, the relatively long cycle times and common use of an autoclave make this method expensive and inappropriate for large volume manufacturing [15]. Furthermore, degradation of the diaphragm material at high temperatures limits which materials can be formed through this method [14]. The high pressures which can be achieved by the hydraulic fluid in hydroforming give the potential to form undercuts, however, the thickness of the diaphragm can limit the size of cavities which can be formed while still achieving good definition of features on the mould [17]. Stamp forming can achieve fast cycle times of 1 min or less [19], leading to high productivity.

Other advantages of stamp forming include that close tolerances can be achieved and high consolidation pressures can be applied during forming [17]. However, there are also some disadvantages including potential thickness mismatch and non-uniform pressure distribution, as well as a high initial tool fabrication cost [17]. Furthermore, stamp forming requires pre-consolidated laminates and the time required for preparing these from pre-preg (using an autoclave or hot pressing) may be significant. Overall, stamp forming is considered the most appropriate thermoforming method for large scale and economical manufacture of components at a high productivity rate.

1.3. A brief history of stamp forming for FRTPs

Stamp forming of FRTPs is similar to the process used in stamp forming of sheet metals [20]. Investigations into stamp forming of FRTPs began in the 1980s, with studies using existing sheet metal forming equipment to shape continuous FRTPs [17]. Later, researchers such as Bigg et al. [21] investigated the solid-state stamping (i.e. forming temperature below T_m but above the matrix glass transition temperature, T_g) of a variety of GF/TPs into trapezoidal and hemispherical parts. Following this, Zahlan et al.

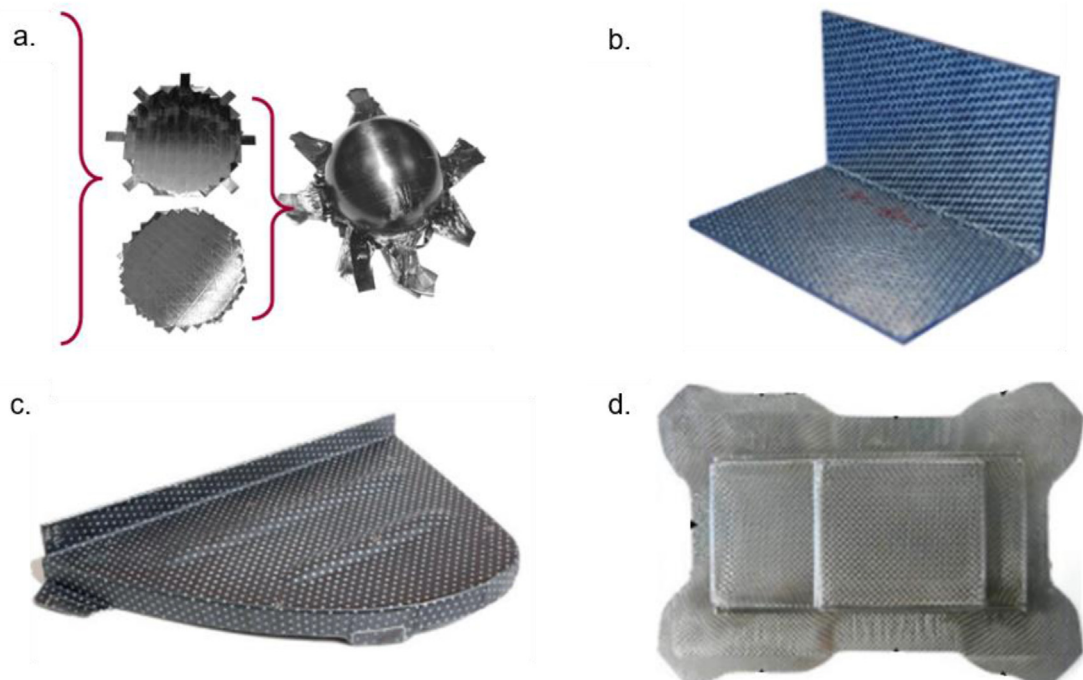


Fig. 3. Example shapes formed by stamp forming: (a) hemisphere, (b) v-shape, (c) wing fixed leading edge stiffener, (d) square cup with two steps [19,29,49,53].

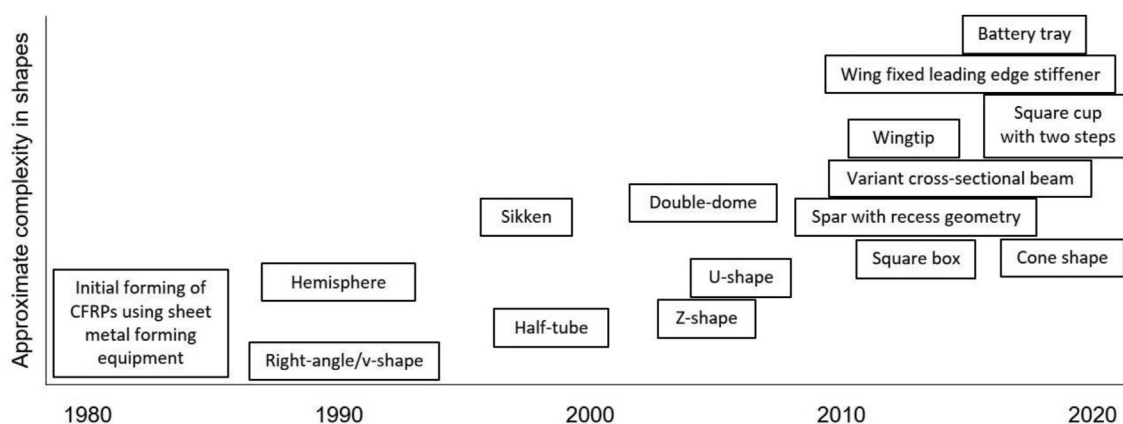


Fig. 4. Development of FRTP shapes/components formed by stamp forming and their approximate complexities [17,23,37–39,41,42,45–47,49,51–54].

[22] formed CF/PEEK into top hat shapes while Hou et al. [23] and Scherer et al. [24] formed CF/polypropylene (CF/PP) into right angle shapes, with the forming temperatures above T_m . Most research focuses on forming at temperatures above T_m and this is the temperature region which is focused on in this review. Hemispheres (Fig. 3(a)) and right angle v-bends (Fig. 3(b)) have commonly been used in forming studies over the years [19,20,25–36]. In recent years, more complex shapes have been formed, including double-domes, u-shapes, variant-cross-sectional-beams, wing fixed leading edge stiffeners (Fig. 3(c)) and boxes with multiple steps (Fig. 3(d)) [37–57]. Fig. 4 summarises the development of different shapes which have been formed through stamp forming since the 1980s. Advancements in the stamp forming process have allowed increasingly complex geometries to be formed, especially during the past decade. Although a mixture of components with flat and curved faces have been successfully formed using stamp forming, each different shape brings slightly different challenges. Therefore, stamp forming processes for a new shape must be carefully designed to reduce defect formation for successful forming of a high quality final part.

2. Mechanisms for stamp forming of FRTPs

2.1. Deformation mechanisms

The four main deformation mechanisms of FRTPs during forming are: resin percolation, transverse flow, inter-ply slip and intra-ply shear [16,58,59]. These mechanisms are shown in Fig. 5, alongside the deformation modes they are required for. The deformation modes increase in complexity moving down Fig. 5 and each one requires not just the deformation mechanism in the same row as it, but also all of the previous deformation mechanisms in the rows above.

Resin percolation is the flow of resin through the fibre network [58], both along and across the fibre direction [59,60], as shown in the first row of Fig. 5. This is required to achieve good consolidation through resin redistribution and the formation of resin-rich interlayers between plies [16]. Resin percolation is mainly dependent on the matrix viscosity, although the lay-up is also important as using different ply orientations will reduce through-thickness permeability (i.e. the ease with which resin can percolate through the fibre structure) compared to having all plies oriented in the same direction [16]. Permeability is higher along the fibre direction compared to the through-thickness direction [16] and is increased for larger diameter fibres due to the larger holes formed between the fibres [60].

Transverse flow occurs when the applied normal pressure forces UD fibres to move in a sideways direction from the centre of the mould [58] or from positions of greater laminate thickness, to which the pressure is applied first [16], to accommodate local pressure variations [59], as shown in the second row of Fig. 5. This occurs due to the uneven pressure distribution which is caused by an uneven laminate surface. Under high pressures, resin flow can also occur along the fibre direction and bleed out of the laminate [16]. This combined with transverse flow can lead to thinning of the plies [16]. Transverse flow is much more significant during forming of UD FRTPs because, in woven FRTPs, transverse flow is restricted by the warp/weft structure [58]. The extent of the mechanism is described by the transverse viscosity [58]. To characterise the transverse flow during forming, parallel-plate “squeeze flow” apparatus can be used [58].

Inter-ply slip involves plies sliding over each other in order to conform to a curved surface [58], as shown in the third row of Fig. 5. The fibres within each ply are assumed to be inextensible, hence the plies must move relative to each other to allow for the different path length of each ply around the curve. For example, when forming a laminate into a bend shape, the inner plies of the bend will be under compression and the outer plies will be under tension. To prevent fibre buckling, inter-ply slip allows the plies to slide over each other and reduce the high compressive stresses in the inner plies. Damage can be controlled in the outer plies as the tensile stresses are also reduced, which will decrease the chance of crack formation. Rotational slip can also occur between the plies when forming doubly-curved surfaces [58] as many parts with complex curvatures require a change in initial fibre direction between adjacent plies [59]. If the stress within each ply is high enough, the shear yield strength (i.e. the stress which must be exceeded for ply slippage to occur) of the resin-rich interlayers can be exceeded, allowing inter-ply slip to take place [14]. The shear yield strength of the interlayer decreases with increasing temperature and, when a certain high temperature above T_m is reached, the thermoplastic matrix can act as a lubricant between the plies and decrease the inter-ply friction [14], facilitating inter-ply slip. The shear stress required for inter-ply slip is dependent on factors including temperature and normal force and is investigated in detail in Section 2.2.1, in which studies characterising ply-ply friction are discussed.

Intra-ply shear occurs within the plane of each ply and allows the material to conform to complex curvature geometries [59]. Fibres are nearly inextensible, therefore, tensile deformations in the fibre direction cannot occur [16,60] for UD FRTPs. Unlike UD FRTPs, woven fabrics can undergo some extension due to their initially


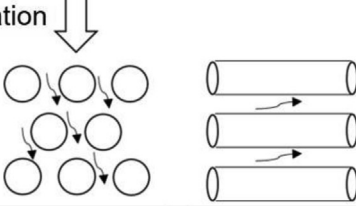

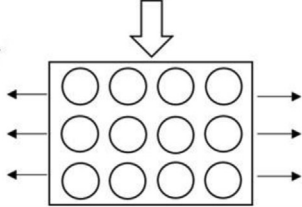
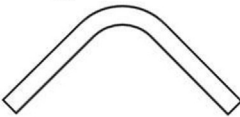
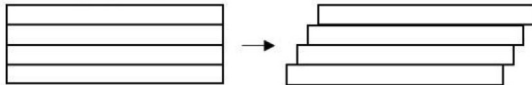
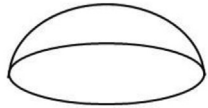
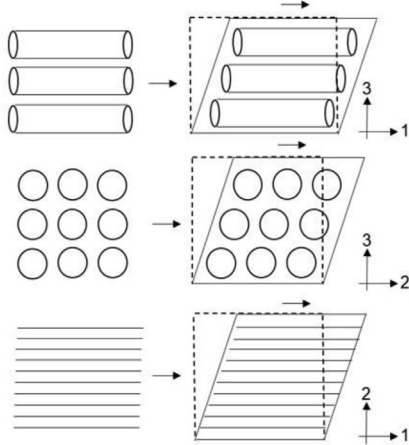
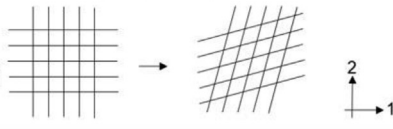
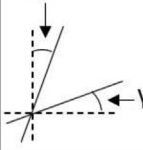
		Deformation mode	Required deformation mechanism
Consolidation	Compliant diaphragm		1. Resin percolation 
	Matched die		1 + 2. Transverse flow 
Shaping	Single curvature		1+2+ 3. Inter-ply slip 
	Double curvature		1+2+3+ 4. Intra-ply shear <div style="display: flex; justify-content: space-around;"> <div style="text-align: center;"> <p>(for UD)</p>  </div> <div style="text-align: center;"> <p>(for woven)</p>  </div> </div> <p>$\gamma/2$</p> 

Fig. 5. Deformation mechanisms required for different deformation modes (adapted from Ref. [16]).

crimped nature. For UD FRTPs, intra-ply shear occurs through individual fibres moving relative to each other [60]. As shown in the fourth row of Fig. 5, for a UD FRTP ply, axial (in 1–3 plane), transverse (in 2–3 plane) and intra-ply shear (in 1–2 plane) can take place [60]. For woven FRTPs, intra-ply shear often occurs through the trellis effect, in which the angle between the two sets of tows in the material changes [58]. This is quantified by the shear angle, γ , which is defined in the fourth row of Fig. 5 [61]. Intra-ply shear in woven FRTPs can be limited when the locking angle (i.e. the angle beyond which the tows cannot rotate any further [58]) of the woven material is reached and further increases in shear strain are not possible [59]. The intra-ply shear behaviour for both cross-ply UD and woven FRTPs can be characterised by bias extension or

picture frame tests [62–64]. Haanappel et al. [65] also proposed a torsion bar test to characterise axial or longitudinal shear in UD FRTPs.

2.2. Friction

Given the requirement for plies to be able to slide over each other during forming and the subsequent importance of inter-ply slip on the deformation process, a clear understanding of inter-ply frictional behaviour is required. Frictional forces present both between plies (known as inter-ply or ply-ply friction) and at the tool-ply interface affect the subsequent deformation. Therefore, the frictional properties at the ply-ply and tool-ply interfaces need to

be characterised to give suitable forming conditions and predictable behaviours, so that the formation of defects such as wrinkles can be avoided. This section provides a comprehensive review of studies from the literature which have investigated the frictional behaviour of FRTPs through a variety of experimental set-ups.

One example of a set-up which can be used to measure inter-ply friction is shown in Fig. 6(a), in which the plies are sandwiched between two metal plates. One ply is pulled out from between two other fixed plies which are under a normal load and have been heated to a certain temperature. A similar set-up which can be used to measure tool-ply friction is shown in Fig. 6(b), in which the fixed plies are removed and one or multiple plies are pulled out from between the metal plates. The pull-out fixture is usually set up on a universal testing machine which provides the pull-out force. Alternative set-ups to measure the friction include a pull-through test arrangement on a universal testing machine [66] or using a sled and plane in accordance with ASTM standard D1894 [67], which was originally designed to measure the frictional behaviour of plastic films.

A load cell in the testing machine measures the pulling force with increase in displacement throughout the pull-out tests. Fig. 7 shows a typical relationship between pull-out force and displacement during a test [68–72]. The pull-out force, F , increases in a relatively linear fashion up until a yield point and then decreases, initially sharply, to reach an approximately steady-state value. The shear stress, τ , can be calculated by taking into account the change of contact area during a test. This is shown in Equation (1), in which A is the instantaneous contact area and F is divided by a factor of two due to there being two contacting surfaces present in the set-up described in Fig. 6 [71]. In ply-ply friction tests, the yield point is related to the shear stress required to initiate ply slippage [68]. In tool-ply friction tests, the yield point has been related to the stress required to break the bond formed between the composite and tool surface during heating prior to the start of slipping [73]. However, Ten Thije et al. [74] observed that the peak friction occurred when the composite is already moving compared to the tool. Therefore, the peak friction may not be identified as a static friction property, but instead as a running-in phenomenon which is not yet fully understood. The friction coefficient, μ , can be calculated using Equation (2), in which N is the normal load, P is the normal pressure and the factor of two is due to there being two contacting surfaces present in the set-up described in Fig. 6 [71]. For an experimental set-up with only one frictional surface, the factor of two is removed from Equations (1) and (2).

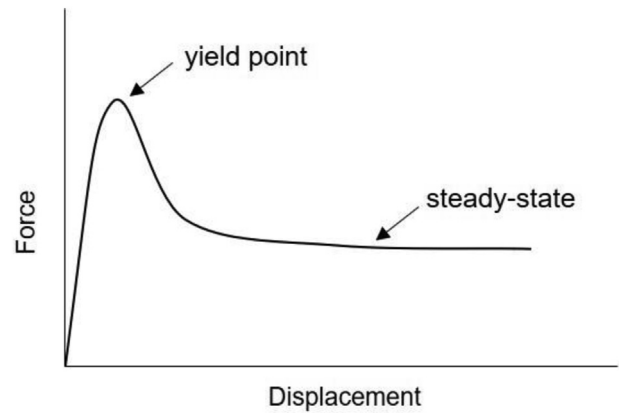


Fig. 7. Typical force-displacement curve for a pull-out test.

The trends for μ and τ with increase in displacement and pressure follow a similar general shape to that for F [70]. As displacement increases, A decreases and N is constant, therefore, P also increases. Hence, increasing displacement is comparable to increasing P . However, in Ref. [70], the approximately steady state region for τ has a slightly positive gradient with increasing P whereas for μ , there appears to be a slightly negative gradient. This is in accordance with Equation (2). Different values for μ can be defined, depending on the part of the pull-out curve the force is taken from. The static coefficient of friction corresponds to the initial peak of the pull-out curve and the dynamic coefficient of friction corresponds to the approximately steady-state pull-out force [71]. Changes in test conditions affect the yield and steady-state shear stresses and the static and dynamic friction coefficients. The subsequent results can be used to determine appropriate forming parameters, such as a suitable temperature for inter-ply slip to occur.

$$\tau = \frac{F/2}{A} \tag{1}$$

$$\frac{F}{2} = \mu N \therefore \mu = \frac{F}{2N} = \frac{\frac{F}{2A}}{\frac{N}{A}} = \frac{\tau}{P} \tag{2}$$

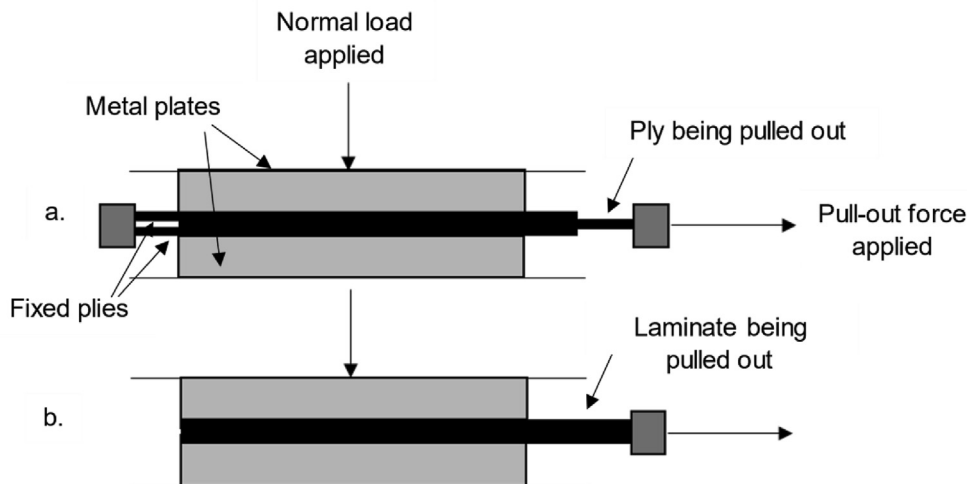


Fig. 6. Example pull-out experiment set-up to measure (a) inter-ply and (b) tool-ply friction.

The friction coefficient, μ , can be related to the Hersey number, H . The Stribeck curve in Fig. 8 demonstrates the variation of μ with H and highlights the different forms of lubrication which can be present. Contacting surfaces are assumed to be fully separated by a fluid film for hydrodynamic lubrication whereas elasto-hydrodynamic lubrication allows for surface deformation [71]. H is a function of resin viscosity, η , speed, U , and normal load, N , as described in Equation (3) [75]. N was originally defined as the normal force per unit width when analysing friction in bearings [75] and this makes H dimensionless. However, studies have since used N (total normal force) [45,71,76–78] or P as the denominator [49,74,79–82]. η is highly temperature dependent, which means μ is related to temperature as well as speed and normal pressure. The complex relationship between μ and various test conditions indicates the need to perform tests on specific materials to establish a clear understanding of frictional behaviour to allow for accurate modelling and successful forming.

$$H = \frac{\eta \cdot U}{N} \tag{3}$$

2.2.1. Ply-ply friction

The ply-ply (or inter-ply) friction behaviour needs to be characterised so that appropriate processing parameters can be chosen for inter-ply slip to occur during forming, which will allow the

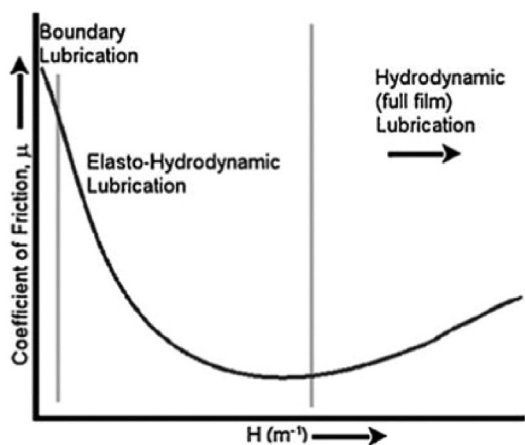


Fig. 8. Stribeck curve [71].

material to conform to the shape of the mould with fewer defects. As well as changing processing parameters, using a thicker resin-rich interlayer can also reduce the shear yield strength [14]. The tests described in the literature have been undertaken on FRTPs at temperatures around or above T_m . The studies investigating inter-ply frictional behaviours are listed in Table 1, with details of the materials used and variables studied. A summary of the trends observed when changing four key parameters (temperature, pressure, pull-out speed and ply orientation) will be given in the following paragraphs.

The yield and steady-state shear stresses decreased with an increase in temperature [14,68–70]. At temperatures above T_m , the resin-rich layer enhances slippage between the plies [68] as the viscosity decreases [14], giving a lower shear stress. At lower temperatures, the viscosity of the matrix increases, giving a more pronounced yield stress [69].

The yield shear stress slightly increased with increasing normal pressure [14]. However, a large normal pressure increase was required to give only a relatively small increase in yield shear stress (i.e. the increase in normal pressure was much larger than the increase in yield shear stress). This led to the ply-ply friction coefficient, μ_{pp} , decreasing as normal pressure increased [69–72], as described by Equation (2). An increased normal pressure may cause increased thinning of the inter-ply resin-rich layer, leading to increased frictional contact between plies [68]. In fabrics, higher normal pressures can increase interlaminar penetration and reduce the thickness of the resin interlayer [69]. This interlaminar penetration can cause interlocking between rovings oriented perpendicular to the direction of slip [70].

Higher yield and steady-state shear stresses were observed for slip between adjacent plies with the same orientation [24,68], as fibres can penetrate from one layer into another when a higher normal pressure is applied [24]. This is because commingling of fibres can occur when adjacent plies have the same orientation and this leads to a lack of a resin-rich layer between the fibres, which can result in a higher inter-ply shear stress as the surface is no longer planar [68]. In contrast, for adjacent plies with different orientations, fibre penetration is much less likely to be possible [24].

Higher yield and steady-state shear stresses were also observed with increasing pull-out speed [68–72,83]. Lebrun et al. [70] found that the pull-out speed had a much greater effect on μ_{pp} and the interlaminar shear stress than the temperature, with the effect becoming more pronounced at higher normal pressures. The decrease in μ_{pp} with increasing pressure was also more pronounced for higher speeds [70]. Additionally, the shear stresses became more rate-dependent at higher temperatures [68].

In summary, inter-ply shear stress increases with:

Table 1
Test conditions in ply-ply friction studies [14,24,68–72,83].

Authors	Material	Temperatures (°C)	Pressures (MPa)	Speeds (mm/min)	Orientations of adjacent plies (°)
Morris et al., 1994 [68]	CF/PEEK UD	324–354	0.62–1	0.762–762	0/0, 0/45, 0/90
Scherer et al., 1990/1991 [24,83]	CF/PP UD	180	Slight	–1–23	0/0, 0/45, 0/90, +45/-45, 45/90, 45/45, 90/90
Lebrun et al., 2004 [70]	GF/PP woven	Preheat: 170–200 Testing: 135–200	0.069–0.28	5–35	N/A
Vanclooster et al., 2008 [69]	GF/PP woven	175–205	0.016–0.063	12.5–400	N/A
Fetfatsidis et al., 2013 [71]	GF/PP woven	Tool: 85 Fabric: 180	0.11–1.033	120–4998	N/A
Bersee et al., 1991 [14]	GF/PEI ^a woven	250–325	1.3–2.0	–	N/A
Akkerman et al., 2010 [72]	GF/PPS + CF/PPS woven	310	0.01–0.05	20–500	N/A

^a Polyetherimide (PEI).

- a decrease in temperature,
- an increase in pressure,
- an increase in speed,
- the use of adjacent plies with the same orientation.

2.2.2. Tool-ply friction

The tool-ply friction needs to be characterised so that the forces acting on the material during deformation can be correctly predicted, allowing accurate modelling and simulation of the forming process. Studies investigating tool-ply frictional behaviour are listed in Table 2, which details the materials used and variables studied. Most tests were undertaken above T_m , although some tests were undertaken at room temperature or at intermediate temperatures. For a non-isothermal test, a low tool temperature may lead to fast cooling of the laminate, meaning that the test does not entirely take place above T_m . This can affect the type of lubrication present.

Some studies observed an increase in tool-ply friction coefficient, μ_{tp} , with an increase in temperature [70,73,79]. However, other studies observed the opposite trend of a decrease in μ_{tp} with increasing temperature [70,74,77,81,84,85], or indeed no significant effect of temperature on friction [80]. The differing results may be due to the different apparatus set-ups and processing parameters used. Lebrun et al. [70] obtained contrasting trends depending on whether the tool temperature was below or above T_m , however, other studies [73,74] obtained contrasting trends, despite both using temperatures above T_m . The temperatures being below or above T_m could have a significant effect on μ_{tp} due to the effect of the presence of liquid on the type of lubrication present. Also, the pressure and speed affect the type of lubrication present which in turn affects μ_{tp} [74]. For temperatures above T_m , the increased temperature may cause a greater contact area between the composite and tool due to softening of the matrix or may reduce the thickness of the resin layer, thus increasing μ_{tp} [73]. Additionally, as matrix viscosity decreases, more fibres are able to penetrate the resin-rich surface layer which increases the Coulomb friction between the tool and the fibres [70]. Alternatively, a higher tool temperature allows a fluid film to remain on the fabric surface for longer, acting as a lubricant and reducing μ_{tp} at higher temperatures [77]. Furthermore, the increased temperature reduces the

matrix viscosity [74] which can improve lubrication and lower μ_{tp} . For temperatures below T_m , fibres cannot penetrate the resin-rich layer so the increase in μ_{tp} with reducing tool temperature may be due to solidification of the matrix and subsequent Coulomb friction between matrix and tool [70]. A cooler tool increases the rate of matrix solidification, leading to an overall increase in μ_{tp} [84]. Lebrun et al. [70] noted that tool-ply shear stress was higher than inter-ply shear stress at higher temperatures, but a transition occurred as temperature dropped, with the tool-ply shear stress becoming lower than the inter-ply shear stress at lower temperatures. The lower tool-ply shear stress compared to inter-ply shear stress at lower temperatures can reduce the chance of fibre breakage during the latter part of the forming process [70]. Based on existing studies, factors such as viscosity, fibre penetration, resin layer thickness and lubrication type appear to dictate the dependence of friction on temperature, but how these factors interact to give a predictable value of μ_{tp} is still not clear. The variability in results from different studies complicates obtaining a consistent understanding of the effect of temperature on tool-ply friction.

A decrease in μ_{tp} was observed for increasing normal loads [70–74,77,79,81,84]. An increased normal load may lead to more resin being squeezed from the centre of the laminate out to the surfaces, increasing the lubrication and decreasing μ_{tp} [77]. The trend observed is consistent with that expected for friction occurring in the hydrodynamic region of the Stribeck curve [71], see Fig. 8 (and Equation (3)), in which it is assumed that the sliding surfaces are completely separated by a fluid film. Additionally, Sachs et al. [80] noted that an increase in pressure made the steady-state friction more velocity dependent and the peak friction less velocity dependent.

A decrease in μ_{tp} for UD ply orientation increasing from 0 to 90° or warp yarn increasing from 0 to 45° from the sliding direction has been observed [72,73,84]. However, some studies concluded that fabric or fibre orientation had no significant influence on μ_{tp} [72,77]. Resin flow across the fibres may be easier than resin flow along the fibre direction, leading to an improvement in lubrication [73]. Also, some materials had more surface warp yarns than weft yarns, resulting in a lower μ_{tp} for sliding in the weft dominant direction [84].

An increase in μ_{tp} was observed for increasing pull-out speeds [71–74,77,80,81,84,85]. The results follow the trend shown in the

Table 2
Test conditions in tool-ply friction studies [70–74,77,79–81,84,85].

Authors	Material	Temperatures (°C)	Pressures (MPa) or Loads (N)	Speeds (mm/min)	Orientations between fibres and pulling direction (°)
Murtagh et al., 1995 [73]	CF/PEEK UD	Isothermal: 25–405	100–750 N	<15–120	0, 90
Sachs et al., 2011 [80]	CF/PEEK UD	Isothermal: 400–420	0.01–0.05 MPa	20–500	N/A
Chow, 2002 [84]	GF/PP woven	Tool: Room-120 Fabric: 100–200	1500–4000 N	1000–2500	0/90, 30/60, 45/45, 90/0 (Warp/Weft)
Gorczyca et al., 2004 [77]	GF/PP woven	Tool: 21–140 Fabric: 160–200	218–4000 N	100.2–4998	0/90, 30/60, 45/45, 60/30, 90/0
Lebrun et al., 2004 [70]	GF/PP woven	Tool: 135–200 Fabric: 170–200	0.069 MPa	20	N/A
Akkerman et al., 2007 [85]	GF/PP woven	Isothermal: 180–220	400–1200 N	20–500	N/A
Ten Thije et al., 2011 [74]	GF/PP woven	Isothermal: 180–220	0.02105–0.06316 MPa	20–500	N/A
Fetfatsidis et al., 2013 [71]	GF/PP woven	Tool: 85 Fabric: 180	0.11–1.033 MPa	120–4998	N/A
Sachs et al., 2014 [81]	GF/PP woven	Isothermal: 23–220 (23 for dry, above 180 for wet)	0.01–0.1 MPa	20–1000	N/A
Akkerman et al., 2010 [72]	GF/PPS and CF/PPS woven	Isothermal: 290–310	0.01–0.05 MPa	20–500	0/90, 90/0
Lee et al., 2017 [79]	CF/PU ^a woven	Isothermal: 110–190	1–5 MPa	600	N/A

^a Polyurethane (PU).

Stribeck curve developed by Ten Thije et al. [74], in which μ_{tp} increases with increasing slipping speed. The trend may also be described by a power-law viscosity model which is able to describe the resin viscosity [77]. The model indicates that, for low speeds, shear stress increases with speed and at high speeds, the shear stress levels off with further increases in speed. The levelling off of μ_{tp} at higher speeds may be due to shear thinning, where resin viscosity decreases at higher speeds, or an increase in thickness of the resin layer due to a layer of transferred polymer building up on the tool surface [73]. Ten Thije et al. [74] observed that the peak friction force was more pronounced at higher speeds. Following the peak, the initially randomly oriented polymers became more oriented as the test progressed, thus μ_{tp} was reduced [74].

In summary, μ_{tp} increases with:

- an increase or decrease in temperature (different conclusions have been obtained),
- a decrease in pressure,
- an increase in speed,
- a decrease in angle between fibre/warp direction and sliding direction.

2.2.3. Friction summary

A summary of the trends seen in the literature between test conditions and shear stress and μ is shown in Table 3. Clearly, the effect of temperature on the tool-ply friction is not universally understood, despite being widely studied. Furthermore, little investigation has taken place regarding the effect of ply orientation on the inter-ply friction of woven composites. The ply-ply and tool-ply friction characteristics of a wide range of materials have not been investigated, with the focus concentrated mainly on woven GF/PP. Wider studies on high performance materials, such as UD and woven CF/PEEK and CF/PPS, are recommended to obtain a consistent understanding of frictional behaviour under a larger range of conditions, given their potential applications in aerospace and automotive industries. Multiple studies are necessary for a detailed understanding of material behaviour due to differences between experimental set-ups across studies. Although the trends from the literature may apply to other materials, the friction characteristics should be investigated prior to stamp forming for each material being used, particularly given the variability in certain conclusions from different studies. Results from these studies can then be used to choose suitable processing parameters for stamp forming, which can be optimised to give good formability and final part quality.

2.3. Consolidation

Several properties constitute the consolidation quality of a material, including void content and interlaminar bond strength [13]. Consolidation quality changes during material processing and

is strongly affected by the thermal and pressure history of the component, such as the pre-consolidation quality of the blank prior to stamp forming [13]. Deconsolidation often occurs when pre-consolidated laminates are heated towards T_m , particularly if little pressure is applied, which can reduce through-thickness heat transfer and increase the required heating time [13,55]. Reasons for deconsolidation include the expansion of dissolved moisture and gas within the matrix and the release of stresses induced during laminate manufacture [44,86]. Therefore, deconsolidation may be reduced through drying of the blanks prior to heating [86].

Once plies have been able to slide against one another to form the required shape, strong bonding between layers is required to achieve good final part quality. The main mechanisms which determine reconsolidation are void collapse and interlaminar bonding [87]. Resin percolation and transverse flow assist these processes [68]. Interlaminar bonding occurs when the molecular chains of the matrix at the ply interface diffuse into the adjacent ply [88]. Over a long enough time, full interpenetration of the chains occurs, meaning the interface is indistinguishable from the bulk polymer. This is called autohesion or self-diffusion. Higher temperatures increase the rate at which this autohesive bond strength reaches the cohesive strength of the bulk polymer [88]. However, autohesive bond formation can only occur if the plies are in intimate contact. Low tow thickness variations within plies are required to achieve good interlaminar bonding at short holding times [87,88]. Short holding times do not allow enough time for the matrix to redistribute and a uniform pressure distribution to be achieved [87]. However, increasing the consolidation pressure can allow blanks with greater thickness variations to be used and still form parts with an acceptable degree of consolidation. Alternatively, the holding time and pressure required for consolidation can be reduced by using pre-preg with a resin-rich surface which enhances matrix redistribution and interlaminar bonding.

3. Challenges and defects

Stamp forming is a complex process and it is a challenge to form defect-free parts. Through understanding the formation mechanisms of defects, the processing parameters can be optimised to reduce the forming defects and improve the final part quality. Common defects include geometric inaccuracies, such as spring-forward, cracks, delaminations, wrinkles and voids. In this section, the latter two defects are discussed in detail.

3.1. Wrinkles

This section gives an overview of wrinkle formation during forming and discusses methods to reduce or eliminate wrinkles. Wrinkles can cause fibre breakage, leading to poor quality final parts. The geometric inaccuracies created might also make parts unsuitable, particularly if a tight tolerance is required. More detailed reviews regarding wrinkles are available in the literature.

Table 3
Effect of increase in process parameters on the ply-ply and tool-ply shear stress and μ .

	Shear stress		μ	
	Ply-ply	Tool-ply	μ_{pp}	μ_{tp}
Temperature	–	+ or –	–	+ or –
Pressure	+	+	–	–
Speed	+	+	+	+
Angle between fibre/warp direction and sliding direction	–	– or unchanged	–	– or unchanged

*+indicates increase, - indicates decrease.

Gereke et al. [89] conducted a review on forming of the textile reinforcement prior to resin infusion, with much focus on wrinkle formation. Boisse et al. [90] gave a review on bending properties and wrinkling of pre-preg during draping simulations.

Out-of-plane buckling and, therefore, wrinkles can occur when fibres are under an in-plane compressive loading condition during deformation [17]. If less energy is required to cause out-of-plane buckling than in-plane deformation, a wrinkle can form [61]. Forming double-curved parts gives a particularly high risk of wrinkle formation [52]. Fig. 9 shows the global laminate deformations observed by Haanappel [91] while forming UD quasi-isotropic laminates into double curvature shapes. If the deformation mode involves only intra-ply shear with some inter-ply slippage, wrinkles will not form (option 1). If this deformation mode presents too much resistance, then a fold can form (option 2). For a material with an adequately low bending stiffness, multiple smaller wrinkles can initially form (option 3), which will then undergo straightening (option 1) or folding (option 2).

In textile fabrics, large in-plane shear strains can also lead to wrinkling, particularly if the shear angle, γ , reaches or exceeds the locking angle [61] (i.e. the angle following which the yarns become in contact with neighbouring yarns and start to laterally compact [93]). In-plane shear stiffness increases at larger shear angles required to form doubly curved parts due to lateral contact between adjacent yarns, increasing the chance of wrinkling [61]. Wrinkles can form when γ exceeds the locking angle because the bending strain energy due to wrinkling is smaller compared to the in-plane shear strain energy (i.e. wrinkle formation has a lower energy dissipation compared to further in-plane deformation) [61]. By forming the wrinkle, the fabric length is increased which reduces the strain energy due to compression. Therefore, out-of-plane wrinkle formation is energetically preferable compared to further in-plane deformation. Furthermore, the formation of wrinkles can also lead to a decrease in the shear angles [61]. However, wrinkling can be mitigated by applying in-plane tension to the material, allowing continued in-plane shear deformation beyond the locking angle without wrinkling. Harrison et al. [64] used biaxial bias extension tests to characterise the onset of wrinkling in woven fabrics and observed that, under increased in-plane tension, γ at onset of wrinkling increased. Therefore, comparing γ to the locking angle cannot be used to predict wrinkle formation alone. Other factors such as tension implemented by

blank holders, in-plane shear and bending energies must be taken into account [61,89,94].

Wrinkle shape is highly dependent on bending stiffness, with higher bending stiffness giving larger wrinkles [61,89,95]. In this way, wrinkle shape is also dependent on temperature as the bending stiffness decreases with increasing temperature. Therefore, the number of wrinkles increases with increasing temperature [95], while their size reduces. The bending properties of the material can be characterised through tests such as the Peirce cantilever, Kawabata bending and three-point bending tests [90]. During cantilever tests conducted on pre-preg in a thermal environmental chamber, the deflection increases with an increase in temperature, confirming a decrease in bending stiffness with increasing temperature, until a point at which the resin is fully melted [95]. At this point the deflection reaches an upper limit, where the fabric (fibre only rather than fibre and matrix) is entirely responsible for the bending stiffness. An accurate value of bending stiffness should be predicted and taken into account, in order to ensure that wrinkles do not extend beyond the excess area and into the final part area, as has occurred in the parts in Fig. 10 [95].

Wrinkling can be reduced by applying in-plane tension to the laminate through constraints such as blank holders [61,89]. This helps prevent the material being under an in-plane compressive stress so reduces the chance of buckling. The buckling and hence the wrinkling behaviour is also affected by the blank shape [96]. Too much excess material forming the flange area can hinder stretching in other parts of the material during deformation, leading to reduced formability [51]. Behrens et al. [52] reduced wrinkling-induced fibre fracture while forming a battery tray with step-geometry and tunnel-geometry by inducing local fibre shear and yarn straightening. Reducing the clamping width near the tunnel area induced yarn straightening in the load direction and local intra-ply fibre shear transverse to the load direction. This kept surplus material out of the tool, which prevented wrinkle formation. Furthermore, fibre fracture was also prevented in part of the mould by using a 45/45° instead of a 0/90° fibre orientation. This choice of material avoided fibres orthogonal to the wrinkle.

Haanappel et al. [49] compared wrinkling during forming of UD CF/PEEK and woven GF/PPS. Although both materials showed similar frictional behaviour, the UD material showed a greater resistance to intra-ply shear. Therefore, the part formed from UD material showed many wrinkles whereas the woven material

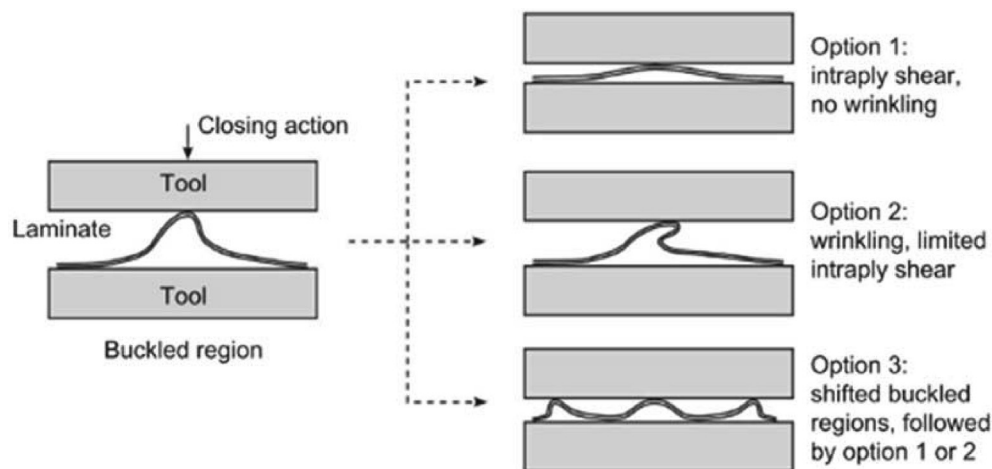


Fig. 9. Laminate deformation behaviours when double curvature leads to excess material during forming [91].

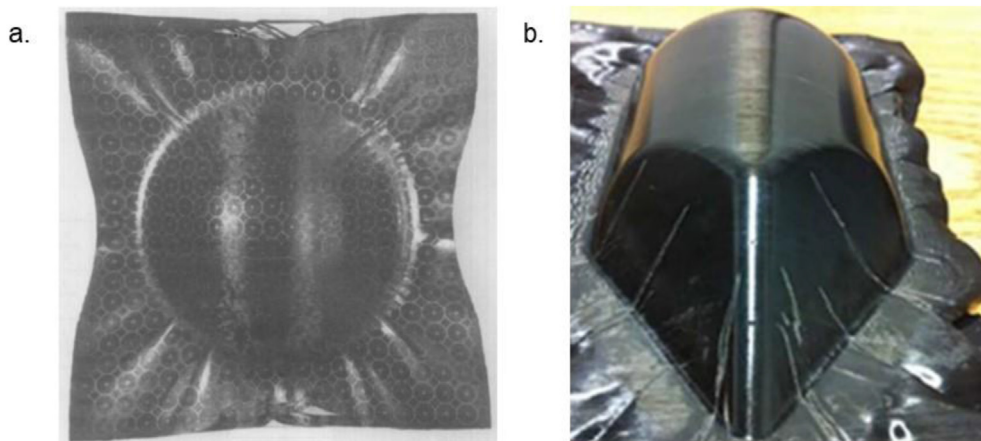


Fig. 10. Wrinkles in final formed parts: (a) hemisphere and (b) shape containing cylindrical portion, quarter sphere and flat faces [56,92].

showed a smooth deformation behaviour. To avoid wrinkle formation when forming a part with double curvature, laminates with more than two unique fibre orientations (such as quasi-isotropic UD laminates) must allow both inter-ply and intra-ply deformation [49,96]. If only two unique fibre orientations are present, intra-ply shear can occur without evoking inter-ply slip if the frictional rigidity is greater than the intra-ply shear rigidity [91,96]. Overall, for forming complex double curved shapes, woven fabrics can more easily form high quality parts than UD material [49,66].

3.2. Voids

Void content has been shown to be directly related to the mechanical properties of formed FRTPs. Liu et al. [97] have written a literature review covering void formation and the effect on mechanical performance in thermoset matrix composites. Some concepts detailed in Liu et al. [97] can also apply for thermoplastic matrix composites.

3.2.1. Formation mechanisms

Voids can form through a number of different mechanisms. One of the most dominant mechanisms is fibre-matrix and interlayer debonding during heating [53], which leads to increasing void formation within the laminate as temperature increases [39], see Fig. 11. This debonding is one of the main contributors to deconsolidation, as explained in Section 2.3. The change in void content can be used as an indication of the degree of thermal deconsolidation [98] and a severe increase in void content can lead to complete delamination of plies [13]. A high processing temperature can reduce the number and size of voids seen in the final part due to the improvement in matrix fluidity, see Fig. 12(a,b). This can

enhance matrix migration and result in void elimination, a more even matrix distribution and improved force transfer and interlayer adhesion [99]. However, at higher temperatures, thermal degradation of the matrix can increase the size of voids [99]. In particular, bar-shaped voids increase in size due to the depletion of interlayer resins [99], see Fig. 12(b,c).

Due to shrinkage of the matrix during cooling, the holding pressure can decline which allows pear-shaped voids to form in resin-rich regions and bar-shaped voids to form in the interlayer due to a lack of resin [99], see Fig. 12(d–f). In addition, voids can also form if air is not fully evacuated from between plies when using unconsolidated material, such as commingled fabrics [100]. Air evacuation can be more difficult when a greater number of plies are used, but this can be mitigated by using a higher temperature which therefore gives a lower matrix viscosity [100]. Moreover, when commingled fibre bundles within a ply are not completely parallel, large regions of resin are required to fill the gaps between the bundles [101]. A lack of matrix in these regions increases the chance of void formation.

3.2.2. Distribution

The distribution of voids changes from being present in both the matrix and fibre-rich regions to being concentrated in fibre-rich regions under higher loading rates and pressures [100]. Fibres within the bundles are compacted together under high pressure, meaning the matrix has more difficulty impregnating the centre of the fibre bundles, leading to voids within the bundles [99]. Jiang et al. [102] found that voids were initially concentrated in the interlaminar region and under increasing pressure void growth occurred along the fibre direction. The overall elongation of the voids slightly increased and the void size, calculated from the

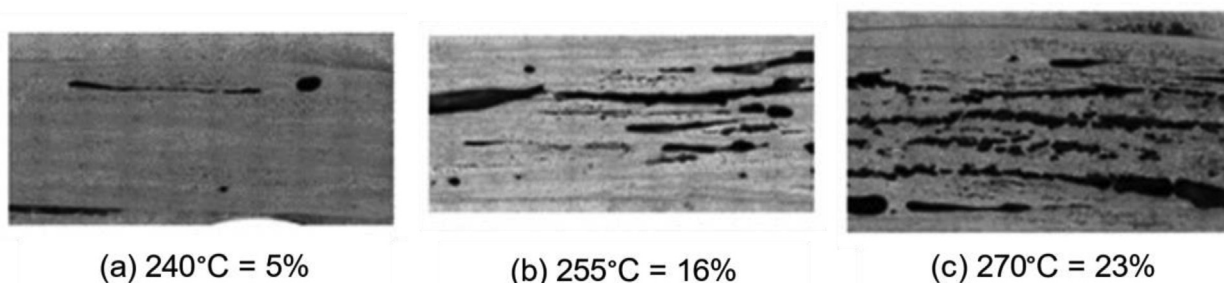


Fig. 11. Void content in GF/PA6 after preheating to: (a) 240 °C, (b) 255 °C and (c) 270 °C [39].

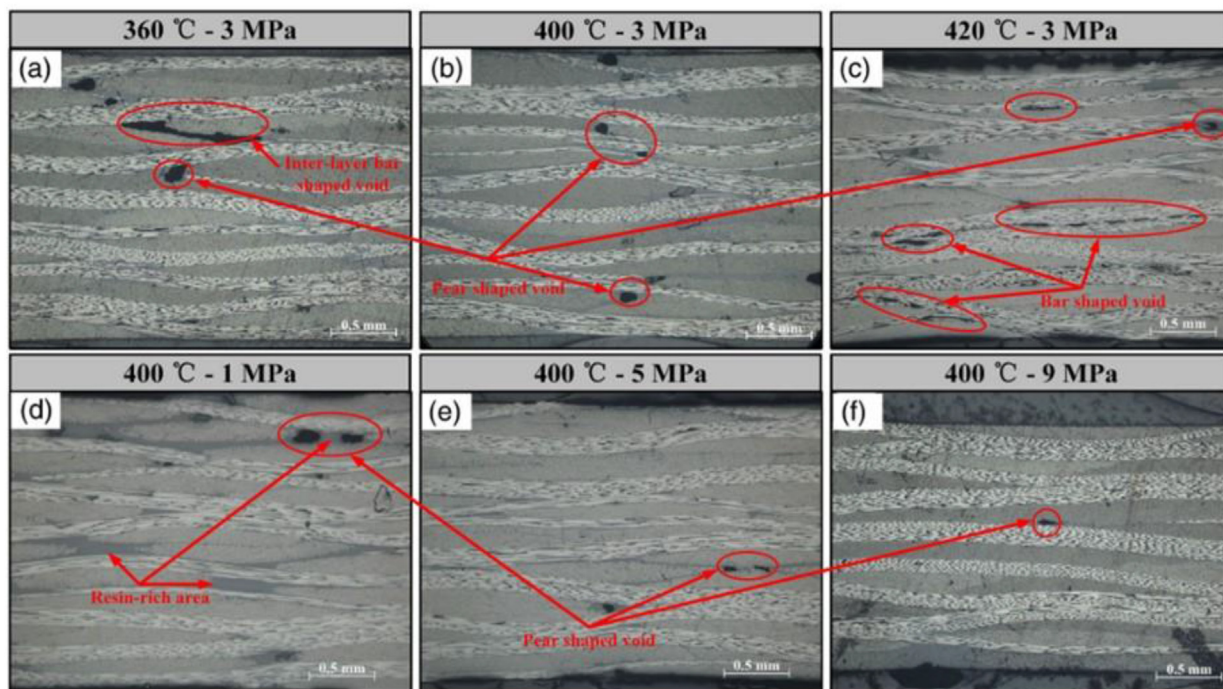


Fig. 12. Microscopic images of woven CF/PEEK laminates fabricated at: (a) 360 °C and 3 MPa, (b) 400 °C and 3 MPa, (c) 420 °C and 3 MPa, (d) 400 °C and 1 MPa, (e) 400 °C and 5 MPa and (f) 400 °C and 9 MPa [99].

average value of the equivalent diameter for each void, slightly decreased, due to the increase in the number of small voids. For longer dwell times, many of the large voids were broken and turned into smaller ones, see Fig. 13. The elongation and flatness of the voids also reduces, with voids becoming more spherical and the equivalent diameter reducing.

3.2.3. Effect on mechanical properties

In general, an increase in void content leads to a reduction in mechanical properties [9,39,99–102]. In particular, matrix-dominated properties such as the flexural strength and modulus and the interlaminar shear strength (ILSS) are strongly affected by void content [100,102]. Subsequently, mechanical properties can be approximated by measuring the void content [100]. Linear relations can be formed between mechanical properties (such as flexural strength and modulus) and void content which allow mechanical properties for components with complex shapes to be approximated [100]. It is difficult to cut specimens of standard dimensions from complex components which have limited flat surfaces, so by measuring the void content, material properties which would otherwise be difficult to measure, can be determined.

Reasons for the deterioration in mechanical properties with an increase in void content include the facts that voids can result in stress concentrations and weaken fibre-matrix and interlaminar bonding. Also, increased void size and content reduces the fracture surface area, which reduces the fracture toughness [101]. Void content changes depending on the processing parameters used and the trends relating void content and mechanical properties to processing parameters are discussed in detail in Section 4.

3.2.4. Void reduction

Intuitively, a high enough pressure must be applied while the matrix is in the molten state to suppress void formation and expansion. Void collapse is an important mechanism to allow good consolidation during stamp forming [87], see Section 2.3. Void reduction strategies are implemented through the determination of optimum forming conditions which can reduce the void content to a level which gives acceptable mechanical properties. Fig. 12 highlights the effect of varying processing parameters (in this case temperature and pressure) on void content and distribution. The effect of the choice of process parameters on final part quality is discussed in detail in Section 4.



Fig. 13. Optical microscopy photographs of the cross section of woven CF/polycarbonate (CF/PC) laminates manufactured at 255 °C and 1 MPa with different dwell times: (a) 5 min, (b) 10 min and (c) 20 min [102].

4. Effect of process parameters on stamp formed parts

In order to find optimum processing conditions for forming high quality parts, an understanding of the effects of different processing parameters on the final part quality is required. To choose specific values for forming parameters, some testing specific to the chosen material or mould shape may be required. For materials which have not previously been studied in detail, preliminary tests to characterise properties such as matrix degradation temperature, T_{deg} , are required. This section presents and compares the findings from forming studies in the literature and allows trends for different parameters to be compared between studies. The current understanding of the effect of processing parameters is summarised. Results from these studies can be used to give an indication of the optimum forming conditions which give the highest quality parts.

4.1. Temperature

Stamping temperature (also known as forming temperature) is dependent on both the laminate and tool temperatures. Cooling of the laminate occurs during transfer from heating source to mould as the large surface area to thickness ratio leads to significant heat loss due to convection [52]. This is followed by cooling of the laminate through conduction upon contact with the cooler mould. Thicker laminates remain at a higher temperature for longer due to their higher thermal capacity, leading to a higher stamping temperature [59]. The change in temperature during forming means that the matrix viscosity also changes, which in turn affects the fibre motion [53] and inter-ply friction. Inter-ply slip is particularly temperature dependent (see Section 2.2.1). Hence, stamping temperature has an important effect on both the formability and the post-form mechanical properties. Therefore, temperature may be considered the most important processing parameter.

Fig. 14 shows the forming temperatures of the matrix materials used by the studies analysed in this section and indicates that most stamp forming studies are conducted at temperatures between T_m and T_{deg} . T_{deg} corresponds to the onset of degradation, which is often defined as the temperature at which 5% or 10% weight loss takes place [108,109]. Therefore, some degradation does occur prior

to this “onset” T_{deg} . However, the matrix may degrade at a different temperature when combined with the fibres, with degradation usually initiating at the fibre/matrix boundary. For example, Zheng et al. [99] observed degradation in woven CF/PEEK at 420 °C, significantly lower than the “onset” T_{deg} of the pure polymer.

Studies in the literature indicate that the tensile, flexural and interlaminar shear strengths (ILSS) of post-form materials increase with increasing forming temperature prior to the onset of matrix degradation [35,99,100,103–105]. There is evidence that flexural modulus may also increase with forming temperature [39,100]. The general trend for tensile strength, ILSS, flexural strength and flexural modulus with variation in temperature is shown in Fig. 15(a).

Higher forming temperatures reduce damage and defect formation and improve consolidation between plies, leading to improvements in mechanical properties. In particular, higher forming temperatures result in lower resin viscosity, which can enhance air evacuation from the laminate [100] and give a more even distribution of resin [99], giving a lower void content and stronger inter-ply adhesion. A higher temperature increases the speed of autohesive bond development between plies, as outlined in Section 2.3.

However, higher forming temperatures can increase the spring-forward effect [29,30,35] and compromise the geometric accuracy of the final part. This is because the larger temperature drop during cooling results in greater anisotropic shrinkage strains [29]. Nevertheless, the shape distortions are mitigated by changes in the mould shape (i.e. mould compensation) or in other processing parameters, such as holding time.

Overall, a higher forming temperature is often beneficial provided that matrix degradation is avoided and that the material does not become too flexible to handle [37]. Therefore, an optimum temperature significantly below T_{deg} but above T_m is preferred.

4.2. Speed

Stamping speed is the speed of the die during forming and can refer to the (initial) closing speed or the compression speed (also called the final closing speed). Initial closing speed is the speed of the die prior to material deformation and compression speed is the speed of the die during material deformation [37,100]. Changing

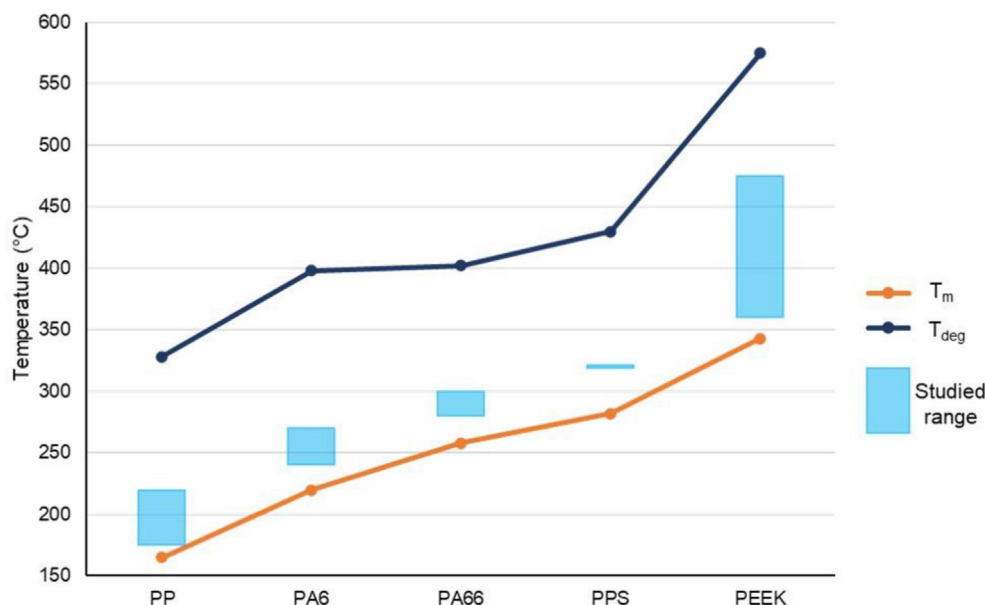


Fig. 14. Studied forming temperatures for different thermoplastic matrices in relation to their melting (T_m) and degradation temperatures (T_{deg}) [29,35,39,55,99,100,103–110].

the initial closing speed affects the amount of heat lost from the laminate due to convective cooling prior to material deformation. The compression speed can affect the viscous forces in the matrix during forming, leading to differing behaviour and damage formation in the laminate [38]. The intra- and inter-ply viscous forces and inter-ply friction forces (see Section 2.2.1) are reduced by using a lower stamping speed, which improves the formability. High stamping speeds can cause severe thinning of the sides of a bend due to resin migration to the outer bend region [111] as well as increasing the damage in the material, such as cracks [33], fibre buckling [16], wrinkling [112] and delamination [36]. In commingled fabrics, high stamping speeds can cause increased tearing and splitting between yarns [113]. However, if using a constant speed for the whole process, the speed must be considered alongside the temperature as using a slower speed to reduce wrinkle formation may actually have the opposite effect due to excessive laminate cooling taking place prior to the final shape being achieved. Hence, stamping speed appears to have a significant effect on the formability, with less of an effect on post-form mechanical properties, unless damage is formed. In this case, poor formability can highly affect post-form mechanical properties.

Trudel-Boucher et al. [100] used a higher initial closing speed until just before the die contacted the material (commingled GF/PP in this study), at which point a slower compression speed was used to force the material into the mould. The use of different speeds reduced the level of material cooling during mould closure and allowed greater accuracy in controlling the displacement of the tool [100]. This study varied loading rate as the equipment used did not allow the pressure to be controlled for constant forming speeds. The effects of loading rate (i.e. the time taken to attain the chosen stamping pressure) and stamping speed (compression speed) are related, but loading rate only refers to the final part of the process, occurring after the main deformation stage. For forming above T_m , flexural strength and modulus increased with loading rate before becoming approximately constant [100]. These properties may decrease slightly at higher loading rates. In contrast, when forming in the solid state (below T_m), Zheng et al. [36] observed that an increase in stamping speed decreased the flexural strength due to increased damage formation [36]. For forming above T_m , void content reduced with increasing loading rate before plateauing [100], demonstrating that a critical loading rate is required to ensure that, prior to the matrix being cooled significantly, sufficient pressure is applied to evacuate the air and wet the fibres. Upon cooling to a certain temperature, the viscosity will increase to a level at which full fibre wetting is impossible. Whether this trend is the same for pre-consolidated laminates (in contrast to the commingled material investigated in Ref. [100]) has not been widely investigated and is unclear. The low void content present in pre-consolidated material prior to heating may make this parameter less important. Furthermore, loading rate relates to the rate at which pressure was applied after the shape had been achieved, so may not give the same trends as stamping speed, which relates to deformation speed. Also, stamping speed affects both void content and formability, but which of these has a greater influence on post-form mechanical properties requires further investigation.

Other processing parameters are partly dependent on the forming speed. A faster speed can lead to a higher pressure [59]. The inertia of the die causes greater compression of the blank due to the higher pressure exerted [23] and, hence, causes a reduced thickness [24]. A faster closing speed leads to an increase in stamping temperature [37,59,114] as there is less time for the sample to lose heat prior to mould closure. Too slow a stamping speed can lead to the laminate temperature decreasing below that required for inter-ply slip to occur [23,111], severely reducing the formability and compromising the final part quality through fibre

buckling and breakage [114]. The general trend for flexural strength and modulus with variation in speed (for forming above T_m) is shown in Fig. 15(b), in which an optimum speed which is fast enough to not allow too much cooling to reduce formability significantly, but slow enough not to create too high viscous and friction forces in the laminate, gives the best mechanical properties.

Overall, a forming speed which is sufficiently slow for excessive resin migration and fibre rupture to be avoided but fast enough to not allow the sample to cool below a workable temperature is preferred. Furthermore, higher speeds increase inter-ply friction, see Section 2.2.1, so a low enough speed to reduce wrinkle formation is also required. Few studies have investigated the effect of forming speed on the mechanical properties of the final part, in particular when using a pre-consolidated laminate as the blank material instead of commingled fabrics, so further detailed study of this is recommended to assist in obtaining optimum stamping speeds. Although a faster forming speed will give a small increase in process cycle time, the holding time is much longer than the stamping time. Therefore, stamping time is not as critical as holding time for overall process cycle time.

4.3. Pressure

During heating, the sheet thickness increases when the matrix becomes molten because of thermal expansion, phase transformation and, in the case of woven fabrics, due to the fibre waviness increasing [53]. This causes de-bonding at the fibre-matrix and layer-layer interfaces, see Section 2.3. Therefore, in addition to forcing the material into the mould, a compression load is required to compress the plies and enhance the consolidation quality, see Section 2.3. Hence, pressure has a great effect on the post-form mechanical properties, in addition to its effect on formability. In particular, the void content is highly dependent on the holding pressure (also known as stamping pressure). The pressure acting on the material during deformation must also be considered due to the increase in inter-ply shear stress caused by higher normal pressures, see Section 2.2.1.

Studies in the literature indicate that post-form flexural strength and ILSS may increase with holding pressure up to a certain level and then decrease or plateau with further pressure increases [99–101,103,115]. Mode I fracture toughness follows the same trend, but mode II fracture toughness continues to improve at higher pressures [101]. The in-plane shear modulus and elongation at failure also increase [100,115]. However, the effects on ILSS are particularly unclear. Dai et al. [103] saw an increase then decrease with pressure increasing up to 3 MPa whereas Zheng et al. [99] saw a slight increase between 1 and 3 MPa, but the change was within the experimental error range. Overall, Zheng et al. [99] observed no significant change with pressure increase up to 9 MPa as void decrease and reduction in interlayer adhesion combined to give an almost unchanged ILSS. Load holding enhances material strength compared to position holding [51,53]. Maintaining the pressure as the sheet shrinks gives a good quality bond strength between fibres and matrix. The general trend for flexural strength, ILSS and Mode I fracture toughness with variation in pressure is shown in Fig. 15(c).

A higher holding pressure promotes re-compaction of the network of fibres and migration of the molten resin into the fibre bundles [99]. This can improve inter-ply and fibre-matrix bonding so may explain the resulting increase in flexural strength and modulus. However, when the pressure is too high, resin overflow occurs along with excessive fibre compression [99,103]. Consequently, it becomes more difficult for resin to flow into the bundles, reducing overall fibre impregnation and hence reducing the capacity for force transmission between fibres and matrix. This can ultimately compromise the mechanical properties.

Overall, an optimum holding pressure must be chosen to give a high level of consolidation while avoiding resin overflow and excessive fibre compression to achieve the optimum mechanical properties. Furthermore, higher normal pressures increase the inter-ply shear stress, see Section 2.2.1, so using a low enough pressure during the deformation stage to reduce wrinkle formation must also be considered for good formability. The relationship between ILSS and holding pressure is not clearly understood, so further studies in this area are recommended.

4.4. Holding time

After the die is closed, the part is usually held in the mould to allow further cooling and consolidation to take place before removal. If the part is removed prior to the completion of matrix solidification, elastic strains in the fibres cannot be arrested [59]. The resulting distortions and shrinkage can give final part shapes which are different to those intended by the mould design. The continued application of pressure while the matrix is still molten allows more time for matrix migration which can improve consolidation quality and reduce void content. This is particularly important for parts formed at relatively lower temperatures and pressures as they require a longer time to achieve good consolidation [19]. Hence, holding time has a significant effect on the post-form mechanical properties and the geometric accuracy of the component.

In general, an increase in holding time appears to improve the ILSS and flexural properties [100,102,103,105]. However, at long holding times no further changes occur. At short holding times, a reduction in flexural strength and modulus may occur if the holding time is less than the solidification time of the matrix [100]. Furthermore, almost identical ILSS values can be obtained for samples moulded at a high temperature with a shorter holding time and those moulded at a lower temperature with a longer holding time [103]. In contrast to samples made from commingled fibres, holding time appears to have little effect on the shear strength of pre-preg due to the strong fibre-matrix interaction already present [105]. Therefore, holding time may be less important for pre-consolidated material. The general trend for flexural strength and modulus and ILSS with variation in holding time is shown in Fig. 15(d).

A reduction in the geometric inaccuracy can be observed with increasing holding time [23,59]. The elastic fibre deformation is not completely prevented if the matrix has not fully solidified. This leads to a distorted cross-section which reduces the final part angle [59]. A solidified matrix can reduce movement of the bent fibres, allowing uniform cross-sections and, hence, uniform parts to be achieved [23].

Overall, too short a holding time can lead to high void contents but too long a holding time can lead to a long processing time. A balance between achieving a low void content and attaining an economical processing time is required to establish an optimum holding time for a given material. A shorter holding time has the benefit of speeding up the manufacturing process and reducing costs as holding time makes up the largest portion of total processing time.

4.5. Cooling rate

The cooling rate experienced by the deformed laminate is dependent on the mould temperature. A higher mould temperature gives a lower cooling rate. Cooling rate is likely to have an effect on the microstructure of the material, particularly the degree of crystallinity which tends to decrease with a higher cooling rate.

This will, in turn, affect the mechanical properties and the amount of volumetric shrinkage. Furthermore, cooling rate is not uniform throughout the material, with greater cooling rates being experienced by surface layers. This reduces the time available for consolidation in these regions which can increase void content [87]. Hence, cooling rate has a great influence on the post-form mechanical properties. In particular, the flexural strength and modulus and fracture toughness are particularly sensitive to cooling rate.

The flexural strength and ILSS generally improve with a decrease in cooling rate [55,105,116–118], as do the elastic and flexural modulus [117–119]. The longitudinal flexural strength is more sensitive to cooling rate than the fibre-dominated longitudinal tensile strength and modulus, given the high dependency on fibre-matrix bonding and matrix strength during bending [117]. Fracture toughness increases with an increase in cooling rate [119,120]. The general trend for flexural strength and modulus, ILSS and elastic modulus with variation in cooling rate is shown in Fig. 15(e). Note that fracture toughness shows the opposite trend to these properties with variation in cooling rate.

The higher degree of crystallinity obtained due to a decreased cooling rate leads to the improvement in strength and modulus [55,118]. Furthermore, a lower cooling rate allows the part to stay molten for longer so gives a more uniform consolidation pressure over the part [55]. This also gives more time for the applied pressure to force the resin into the fibre bundles. Therefore, more entanglement occurs between the molecular chains and the fibres, improving the interfacial bond strength [118]. Slow cooling forms more closely packed crystalline lamellae in the fibre-matrix interphase region, imparting strong fibre-matrix interfacial bonds which undergo debonding in a relatively brittle manner [116,117]. The stress transfer between fibre and matrix is increased by the thicker crystalline region around the fibre [121]. Faster cooling forms more amorphous regions of polymer which form a much weaker fibre-matrix interfacial bond and undergo ductile failure [116,117]. Although the improvement in fracture toughness is due to extensive matrix plasticity, the increased matrix ductility may not lead to as great an increase in fracture toughness as might be expected, because of premature interface debonding resulting from the reduced fibre-matrix interfacial strength [120].

Overall, lower cooling rates tend to give superior flexural and shear properties, although, the fracture toughness can be reduced. However, lower cooling rates lead to increased processing times and hence make manufacturing more expensive. An optimum compromise must be made based on the required material properties and application to give an appropriate cooling rate for processing.

4.6. Effect of process parameters summary

A summary of the effect of an increase in certain processing parameters on a selection of post-form mechanical and physical properties is shown in Table 4. Fig. 15 demonstrates visually the general trends of increasing certain processing parameters on a selection of mechanical properties. It should also be noted that some of these independent trends are actually highly interdependent on other processing parameters. For example, the applied pressure will affect the required holding time and using too low a pressure may change the indicated holding time trend. Furthermore, these trends assume a certain temperature is reached, e.g. for temperatures significantly below T_m , stamp forming cannot take place and the effect of these parameters becomes irrelevant.

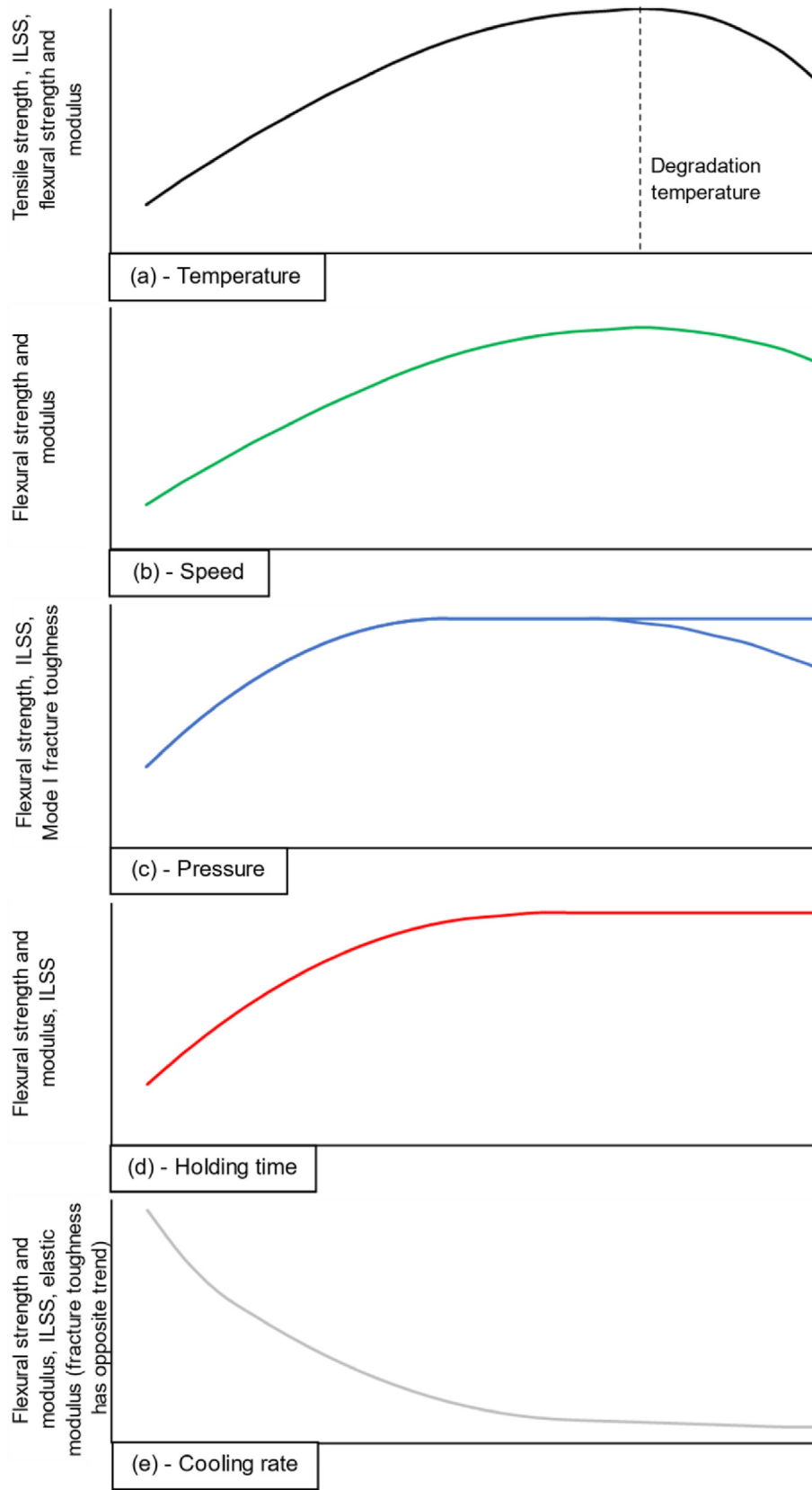


Fig. 15. General trends of the effect of an increase in a certain processing parameter on some post-form material properties. Increase in: (a) - temperature, (b) - speed, (c) - pressure, (d) - holding time, (e) - cooling rate [35,39,55,99–105,115–119].

Table 4
Effect of an increase in certain processing parameters on a selection of mechanical and physical properties.

	Tensile strength	Flexural strength and modulus	ILSS	Fracture toughness	Void content
Temperature	+	+	+	+	–
Speed		+			–
Pressure	+	+	+ or unchanged	+	–
Holding time		+	+		–
Cooling rate	–	–	–	+	+

*+ indicates increase, - indicates decrease.

5. Conclusion

This review provides an extensive survey of current fibre-reinforced thermoplastic (FRTP) stamp forming technology. A comprehensive analysis of the deformation mechanisms, the frictional behaviour and the formation of defects in FRTPs during stamp forming, as well as the effect of different processing parameters on mechanical properties of as-formed parts, has been conducted. Major forming defects, including wrinkles and voids, have been discussed. Void content has a large influence on resulting mechanical properties so must be minimised as part of optimising the process parameters. Wrinkling remains a challenge during stamp forming but can be minimised through a detailed knowledge of material behaviour and the use of computational modelling and simulations. The main findings of this review are summarised below.

It is concluded that inter-ply shear stress increases with a decrease in temperature, an increase in pressure or speed, or having adjacent plies with the same orientation. Further friction studies on high performance FRTPs, such as CF/PEEK and CF/PPS, are recommended, particularly at a wider range of test temperatures. These materials offer significant potential in aerospace and automotive applications. Therefore, a detailed understanding of their behaviours during stamp forming can pave the way to high quality and economical production of parts.

Higher temperatures can lower the probability of wrinkle formation and give better mechanical properties through reducing voids and improving consolidation. However, the temperature must remain below the temperature for the onset of matrix degradation (T_{deg}). Higher forming speeds can increase the chance of wrinkle formation, but may prevent excessive laminate cooling prior to the completion of forming. Higher pressures increase the inter-ply friction but improve post-form mechanical properties through improved consolidation and void reduction, although excessive pressure must be avoided to prevent resin overflow and excessive fibre compression. Longer holding times lower the void content but increase the cycle time and cost of the manufacturing process. Higher cooling rates can improve toughness but reduce other post-form material properties, allowing a suitable cooling rate to be chosen based on the required mechanical properties for a specific application. Determining the optimum processing parameters which give the most desirable post-form mechanical properties and processing time for a particular material and part requires a systematic study of the material and a thorough understanding of the aforementioned factors. Relatively few studies have directly investigated the effect of forming speed on the post-form mechanical properties, so more detailed study of this is also recommended.

With further developments in understanding of FRTP material behaviour under stamp forming conditions, the manufacture of increasingly complex shapes at reasonable costs is possible. This will increase the number of applications for FRTP parts in the transport industry, allowing improved efficiencies and emissions targets to be reached. Investigating more extensive material

constituents, such as new thermoplastic matrices, may push the current boundaries for structural performance, manufacturability and cost to new levels.

Conflicts of interest

The authors declare that there is no conflicts of interest.

Acknowledgments

Hongyan Wang acknowledges the support from the Chinese Scholarship Council (CSC) and Imperial College for the CSC Imperial Scholarship; Zerong Ding acknowledges the support from the Shougang-Imperial Joint Laboratory.

References

- [1] A. Mahashabde, P. Wolfe, A. Ashok, C. Dorbian, Q. He, A. Fan, et al., Assessing the environmental impacts of aircraft noise and emissions, *Prog. Aero. Sci.* 47 (1) (2011) 15–52. Available from: <https://doi.org/10.1016/j.paerosci.2010.04.003>.
- [2] European Union, Setting CO2 Emission Performance Standards for New Passenger Cars and for New Light Commercial Vehicles, and Repealing Regulations (EC) No 443/2009 and (EU) No 510/2011, 2019.
- [3] G. Hellard, Composites in Airbus: a long story of innovations and experiences, in: Airbus Global Investor Forum. Seville, 2008. Available from: <https://docplayer.net/25342669-Composites-in-airbus-a-long-story-of-innovations-and-experiences-presented-by-guy-hellard.html>.
- [4] Boeing, Advanced composite use [internet] [cited 2021 May 6]. Available from: <https://www.boeing.com/commercial/787/by-design/#/advanced-composite-use>.
- [5] M. Marino, R. Sabatini, Advanced lightweight Aircraft design configurations for green operations, in: Practical Responses to Climate Change Conference 2014. Melbourne, 2014, pp. 207–215. Available from: https://researchrepository.rmit.edu.au/discovery/fulldisplay/alma9921862409301341/61RMIT_INST:ResearchR%0Ahttp://researchbank.rmit.edu.au/view/rmit:30631.
- [6] M. Such, C. Ward, K. Potter, Aligned discontinuous fibre composites: a short history, *J. Multifunc. Comp.* 2 (3) (2014) 155–168.
- [7] P. Bussetta, N. Correia, Numerical forming of continuous fibre reinforced composite material: a review, *Compos. Appl. Sci. Manuf.* 113 (2018) 12–31. Available from: <https://doi.org/10.1016/j.compositesa.2018.07.010>.
- [8] F.L. Matthews, R.D. Rawlings, *Composite Materials: Engineering and Science*, Woodhead Publishing Ltd, Cambridge, 1999.
- [9] L. Ye, K. Friedrich, J. Kästel, Y.W. Mai, Consolidation of unidirectional CF/PEEK composites from commingled yarn prepreg, *Compos. Sci. Technol.* 54 (4) (1995) 349–358. Available from: [https://doi.org/10.1016/0266-3538\(95\)00061-5](https://doi.org/10.1016/0266-3538(95)00061-5).
- [10] H. Liu, J. Liu, Y. Ding, J. Zheng, X. Kong, J. Zhou, et al., The behaviour of thermoplastic and thermoset carbon fibre composites subjected to low-velocity and high-velocity impact, *J. Mater. Sci.* 55 (2020) 15741–15768. Available from: <https://doi.org/10.1007/s10853-020-05133-0>.
- [11] R.A. Witik, R. Teuscher, V. Michaud, C. Ludwig, J.A.E. Manson, Carbon fibre reinforced composite waste: an environmental assessment of recycling, energy recovery and landfilling, *Compos. Appl. Sci. Manuf.* 49 (2013) 89–99. Available from: <https://doi.org/10.1016/j.compositesa.2013.02.009>.
- [12] F. Sacchetti, W.J.B. Grove, L.L. Warnet, I.F. Villegas, Effect of resin-rich bond line thickness and fibre migration on the toughness of unidirectional Carbon/PEEK joints, *Compos. Appl. Sci. Manuf.* 109 (February) (2018) 197–206. Available from: <https://doi.org/10.1016/j.compositesa.2018.02.035>.
- [13] T.K. Slange, L. Warnet, W.J.B. Grove, R. Akkerman, Influence of pre-consolidation on consolidation quality after stamp forming of C/PEEK composites, in: AIP Conference Proceedings 1769 (1) (2016) 170022. Available from: <https://doi.org/10.1063/1.4963578>.

- [14] H.E.N. Bersee, L.M.J. Robroek, The role of the thermoplastic matrix in forming processes of composite materials, *Compos. Manuf.* 2 (3–4) (1991) 217–222. Available from: [https://doi.org/10.1016/0956-7143\(91\)90143-5](https://doi.org/10.1016/0956-7143(91)90143-5).
- [15] A.C. Long (Ed.), *Composites Forming Technologies*, Woodhead Publishing Ltd, Cambridge, 2007.
- [16] F.N. Cogswell, *Thermoplastic Aromatic Polymer Composites*. Melksham, Butterworth-Heinemann Ltd, Wiltshire, 1992.
- [17] R.K. Okine, Analysis of forming parts from advanced thermoplastic composite sheet materials, *J. Thermoplast. Compos. Mater.* 2 (1) (1989) 50–76. Available from: <https://doi.org/10.1177/F089270578900200104>.
- [18] J. Krebs, K. Friedrich, D. Bhattacharyya, A direct comparison of matched-die versus diaphragm forming, *Compos. Appl. Sci. Manuf.* 29 (1–2) (1998) 183–188. Available from: [https://doi.org/10.1016/S1359-835X\(97\)82706-6](https://doi.org/10.1016/S1359-835X(97)82706-6).
- [19] A. Burkhardt, D. Cramer, Feasibility of continuous-fiber reinforced thermoplastic tailored blanks for automotive applications, in: *5th SPE Automotive Composites Conference & Exhibition*, 2005, pp. 1–9.
- [20] S.F. Hwang, K.J. Hwang, Stamp forming of locally heated thermoplastic composites, *Compos. Appl. Sci. Manuf.* 33 (5) (2002) 669–676. Available from: [https://doi.org/10.1016/S1359-835X\(02\)00004-0](https://doi.org/10.1016/S1359-835X(02)00004-0).
- [21] D.M. Bigg, J.R. Preston, Thermoplastic matrix composites, *Polym. Compos.* 10 (4) (1989) 261–268. Available from: <https://doi.org/10.1002/pc.750100409>.
- [22] N. Zahlan, J.M. O'Neill, Design and fabrication of composite components; the spring-forward phenomenon, *Composites* 20 (1) (1989) 77–81, [https://doi.org/10.1016/0010-4361\(89\)90685-X](https://doi.org/10.1016/0010-4361(89)90685-X). Available from: .
- [23] M. Hou, K. Friedrich, Stamp forming of continuous carbon fibre/polypropylene composites, *Compos. Manuf.* 2 (1) (1991) 3–9. Available from: [https://doi.org/10.1016/0956-7143\(91\)90153-8](https://doi.org/10.1016/0956-7143(91)90153-8).
- [24] R. Scherer, K. Friedrich, Inter- and intraply-slip flow processes during thermoforming of CF/PP-laminates, *Compos. Manuf.* 2 (2) (1991) 92–96, [https://doi.org/10.1016/0956-7143\(91\)90185-J](https://doi.org/10.1016/0956-7143(91)90185-J). Available from: .
- [25] M.D. Wakeman, L. Zingraff, P.E. Bourban, J.A.E. Manson, P. Blanchard, Stamp forming of carbon fibre/PA12 composites - a comparison of a reactive impregnation process and a commingled yarn system, *Compos. Sci. Technol.* 66 (1) (2006) 19–35. Available from: <https://doi.org/10.1016/j.compscitech.2005.06.001>.
- [26] B.C. Meyer, Ch v. Katsiropoulos, SpG. Pantelakis, Hot forming behavior of non-crimp fabric peek/c thermoplastic composites, *Compos. Struct.* 90 (2) (2009) 225–232. Available from: <https://doi.org/10.1016/j.compstruct.2009.03.013>.
- [27] S.P. Haanappel, R ten Hijne, R. Akkerman, Forming Predictions of Ud Reinforced Thermoplastic Laminates, in: *14th European Conference on Composite Materials*, 2010, pp. 1–10. June.
- [28] P. Han, J. Butterfield, M. Price, A. Murphy, M. Mullin, N. Ireland, Part Form Prediction Methods for Carbon Fibre, in: *18th International Conference on Composite Materials*, 2011.
- [29] P. Han, J. Butterfield, M. Price, S. Buchanan, A. Murphy, Experimental investigation of thermoforming carbon fibre-reinforced polyphenylene sulphide composites, *J. Thermoplast. Compos. Mater.* 28 (4) (2013) 529–547. Available from: <https://doi.org/10.1177/0892705713486133>.
- [30] P. Han, J. Butterfield, S. Buchanan, R. McCool, Z. Jiang, M. Price, et al., The prediction of process-induced deformation in a thermoplastic composite in support of manufacturing simulation, *Proc. IME B J. Eng. Manufact.* 227 (10) (2013) 1417–1429. Available from: <https://doi.org/10.1177/0954405413488362>.
- [31] S. Davey, R. Das, W.J. Cantwell, S. Kalyanasundaram, Forming studies of carbon fibre composite sheets in dome forming processes, *Compos. Struct.* 97 (2013) 310–316. Available from: <https://doi.org/10.1016/j.compstruct.2012.10.026>.
- [32] Y. Uriya, K. Ikeuch, J. Yanagimoto, Cold and warm V-bending test for carbon-fiber-reinforced plastic sheet, *Procedia Eng.* 81 (October) (2014) 1633–1638. Available from: <https://doi.org/10.1016/j.proeng.2014.10.203>.
- [33] Q. Zhang, Q. Gao, J. Cai, Experimental and simulation research on thermal stamping of carbon fiber composite sheet, *Trans. Nonferrous Metals Soc. China* 24 (1) (2014) 217–223. Available from: [https://doi.org/10.1016/S1003-6326\(14\)63050-8](https://doi.org/10.1016/S1003-6326(14)63050-8).
- [34] A. Gherissi, F. Abbassi, A. Ammar, A. Zghal, Numerical and experimental investigations on deep drawing of G1151 carbon fiber woven composites, *Appl. Compos. Mater.* 23 (3) (2016) 461–476, <https://doi.org/10.1007/s10443-015-9468-x>. Available from: .
- [35] G.Y. Fortin, G. Fernlund, Effect of tool temperature on dimensional fidelity and strength of thermoformed polyetheretherketone composites, *Polym. Compos.* 40 (11) (2019) 4376–4389. Available from: <https://doi.org/10.1002/pc.25300>.
- [36] B. Zheng, X. Gao, M. Li, T. Deng, Z. Huang, H. Zhou, et al., Formability and failure mechanisms of woven CF/PEEK composite sheet in solid-state thermoforming, *Polymers* 11 (6) (2019) 966. Available from: <https://doi.org/10.3390/polym11060966>.
- [37] K. Friedrich, M. Hou, On stamp forming of curved and flexible geometry components from continuous glass fiber/polypropylene composites, *Compos. Appl. Sci. Manuf.* 29 (3) (1998) 217–226. Available from: [https://doi.org/10.1016/S1359-835X\(97\)00087-0](https://doi.org/10.1016/S1359-835X(97)00087-0).
- [38] P. de Luca, P. Lefébure, A.K. Pickett, Numerical and experimental investigation of some press forming parameters of two fibre reinforced thermoplastics: APC2-AS4 and PEI-CETEX, *Compos. Appl. Sci. Manuf.* 29 (1–2) (1998) 101–110. Available from: [https://doi.org/10.1016/S1359-835X\(97\)00060-2](https://doi.org/10.1016/S1359-835X(97)00060-2).
- [39] M.D. Wakeman, P. Blanchard, J.A.E. Manson, Void evolution during stamp-forming of thermoplastic composites, *SAVE Proc.* 1001 (July) (2005) 15.
- [40] P. Harrison, R. Gomes, N. Curado-Correia, Press forming a 0/90 cross-ply advanced thermoplastic composite using the double-dome benchmark geometry, *Compos. Appl. Sci. Manuf.* 54 (2013) 56–69. Available from: <https://doi.org/10.1016/j.compositesa.2013.06.014>.
- [41] D. Soulat, A. Cheruet, P. Boisse, Simulation of continuous fibre reinforced thermoplastic forming using a shell finite element with transverse stress, *Comput. Struct.* 84 (13–14) (2006) 888–903. Available from: <https://doi.org/10.1016/j.compstruc.2006.02.011>.
- [42] A. Salomi, T. Garstka, K. Potter, A. Greco, A. Maffezzoli, Spring-in angle as molding distortion for thermoplastic matrix composite, *Compos. Sci. Technol.* 68 (14) (2008) 3047–3054. Available from: <https://doi.org/10.1016/j.compscitech.2008.06.024>.
- [43] J.S. Lightfoot, M.R. Wisnom, K. Potter, A new mechanism for the formation of ply wrinkles due to shear between plies, *Compos. Appl. Sci. Manuf.* 49 (2013) 139–147. Available from: <https://doi.org/10.1016/j.compositesa.2013.03.002>.
- [44] V. Donadei, F. Lionetto, M. Wielandt, A. Offringa, A. Maffezzoli, Effects of blank quality on press-formed PEKK/carbon composite parts, *Materials* 11 (7) (2018) 1063. Available from: <https://doi.org/10.3390/ma11071063>.
- [45] P. Wang, N. Hamila, P. Boisse, Thermoforming simulation of multilayer composites with continuous fibres and thermoplastic matrix, *Compos. B Eng.* 52 (2013) 127–136. Available from: <https://doi.org/10.1016/j.compositesb.2013.03.045>.
- [46] H. Yin, X. Peng, T. Du, J. Chen, Forming of thermoplastic plain woven carbon composites: an experimental investigation, *J. Thermoplast. Compos. Mater.* 28 (5) (2013) 730–742. Available from: <https://doi.org/10.1177/0892705713503668>.
- [47] P. Hallander, M. Akermo, C. Mattei, M. Petersson, T. Nyman, An experimental study of mechanisms behind wrinkle development during forming of composite laminates, *Compos. Appl. Sci. Manuf.* 50 (2013) 54–64. Available from: <https://doi.org/10.1016/j.compositesa.2013.03.013>.
- [48] S. Hineno, T. Yoneyama, D. Tatsuno, M. Kimura, K. Shiozaki, T. Moriyasu, et al., Fiber deformation behavior during press forming of rectangle cup by using plane weave carbon fiber reinforced thermoplastic sheet, *Procedia Eng.* 81 (October) (2014) 1614–1619. Available from: <https://doi.org/10.1016/j.proeng.2014.10.199>.
- [49] S.P. Haanappel, R.H.W. ten Hijne, U. Sachs, B. Rietman, R. Akkerman, Formability analyses of uni-directional and textile reinforced thermoplastics, *Compos. Appl. Sci. Manuf.* 56 (2014) 80–92. Available from: <https://doi.org/10.1016/j.compositesa.2013.09.009>.
- [50] T. Joppich, D. Doerr, L. van der Meulen, T. Link, B. Hangs, F. Henning, Layup and process dependent wrinkling behavior of PPS/CF UD tape-laminates during non-isothermal press forming into a complex component, *AIP Conf. Proc.* 1769 (1) (2016) 170012. Available from: <https://doi.org/10.1063/1.4963568>.
- [51] D. Tatsuno, T. Yoneyama, K. Kawamoto, M. Okamoto, Production system to form, cut, and join by using a press machine for continuous carbon fiber-reinforced thermoplastic sheets, *Polym. Compos.* 39 (7) (2016) 2571–2586. Available from: <https://doi.org/10.1002/pc.24242>.
- [52] B.A. Behrens, A. Raatz, S. Hübner, C. Bonk, F. Bohne, C. Bruns, et al., Automated stamp forming of continuous fibre reinforced thermoplastics for complex shell geometries, in: J. Fleischer, R. Teti (Eds.), *Procedia CIRP*, 2017, pp. 113–118. Available from: <https://doi.org/10.1016/j.procir.2017.03.294>.
- [53] D. Tatsuno, T. Yoneyama, K. Kawamoto, M. Okamoto, Hot press forming of the thermoplastic FRP sheets, *Procedia Manuf.* 15 (2018) 1730–1737. Available from: <https://doi.org/10.1016/j.promfg.2018.07.254>.
- [54] T. Zenker, S. Schön, Stamp forming of thermoplastic automated fiber placement blanks: influence of layup parameters on part quality, *AIP Conf. Proc.* 2113 (1) (2019) 20021. Available from: <https://doi.org/10.1063/1.5112526>.
- [55] H. Lessard, G. Lebrun, A. Benkaddour, X.T. Pham, Influence of process parameters on the thermostamping of a [0/90]₁₂ carbon/polyether ether ketone laminate, *Compos. Appl. Sci. Manuf.* 70 (2015) 59–68. Available from: <https://doi.org/10.1016/j.compositesa.2014.12.009>.
- [56] A. Benkaddour, G. Lebrun, L. Laberge-Lebel, Thermostamping of [0/90]_n carbon/peek laminates: influence of support configuration and demolding temperature on part consolidation, *Polym. Compos.* 39 (9) (2018) 3341–3352. Available from: <https://doi.org/10.1002/pc.24354>.
- [57] A. Schug, Unidirectional fibre reinforced thermoplastic composites: a forming study, 2020. Available from: <https://mediatum.ub.tum.de/doc/1469957/1469957.pdf>.
- [58] A.M. Murtagh, P.J. Mallon, Characterisation of shearing and frictional behaviour during sheet forming, in: D. Bhattacharyya (Ed.), *Composite Sheet Forming*, in *Composite Materials Series*, Elsevier, 1997, pp. 163–216.
- [59] K. Friedrich, M. Hou, J. Krebs, Thermoforming of continuous fibre/thermoplastic composite sheets, in: D. Bhattacharyya (Ed.), *Composite Sheet Forming*, in *Composite Materials Series*, Elsevier, 1997, pp. 91–162.
- [60] F.N. Cogswell, The experience of thermoplastic structural composites during processing, *Compos. Manuf.* 2 (3–4) (1991) 208–216. Available from: [https://doi.org/10.1016/0956-7143\(91\)90142-4](https://doi.org/10.1016/0956-7143(91)90142-4).
- [61] P. Boisse, N. Hamila, E. Vidal-Sallé, F. Dumont, Simulation of wrinkling during textile composite reinforcement forming. Influence of tensile, in-plane shear and bending stiffnesses, *Compos. Sci. Technol.* 71 (5) (2011) 683–692. Available from: <https://doi.org/10.1016/j.compscitech.2011.01.011>.

- [62] K. Potter, Bias extension measurements on cross-ply unidirectional thermoset prepreg, *Compos. Appl. Sci. Manuf.* 33 (1) (2002) 63–73. Available from: [https://doi.org/10.1016/S1359-835X\(01\)00057-4](https://doi.org/10.1016/S1359-835X(01)00057-4).
- [63] J. Sjölander, P. Hallander, M. Akermo, Forming induced wrinkling of composite laminates: a numerical study on wrinkling mechanisms, *Compos. Appl. Sci. Manuf.* 81 (2016) 41–51. Available from: <https://doi.org/10.1016/j.compositesa.2015.10.012>.
- [64] P. Harrison, F. Abdiwi, Z. Guo, P. Potluri, W.R. Yu, Characterising the shear-tension coupling and wrinkling behaviour of woven engineering fabrics, *Compos. Appl. Sci. Manuf.* 43 (6) (2012) 903–914. Available from: <https://doi.org/10.1016/j.compositesa.2012.01.024>.
- [65] S.P. Haanappel, R. Akkerman, Shear characterisation of uni-directional fibre reinforced thermoplastic melts by means of torsion, *Compos. Appl. Sci. Manuf.* 56 (2014) 8–26. Available from: <https://doi.org/10.1016/j.compositesa.2013.09.007>.
- [66] U. Sachs, Friction and bending in thermoplastic composites forming processes, PhD thesis, 2014.
- [67] ASTM International, Standard test method for static and kinetic coefficients of friction of plastic film and sheeting (D 1894 - 01) [internet], West conshohocken, PA, 2014, pp. 1–7. Available from: <https://compass.astm.org/download/D1894.14629.pdf>.
- [68] S.R. Morris, C.T. Sun, An investigation of interply slip behaviour in AS4/PEEK at forming temperatures, *Compos. Manuf.* 5 (4) (1994) 217–224. Available from: [https://doi.org/10.1016/0956-7143\(94\)90136-8](https://doi.org/10.1016/0956-7143(94)90136-8).
- [69] K. Vanclooster, S.V. Lomov, I. Verpoest, Investigation of interply shear in composite forming, *Int. J. Material Form.* 1 (2008) 185–188. Available from: <https://doi.org/10.1007/s12289-008-0022-3>.
- [70] G. Lebrun, M.N. Bureau, J. Denault, Thermoforming-stamping of continuous glass fiber/polypropylene composites: interlaminar and tool-laminate shear properties, *J. Thermoplast. Compos. Mater.* 17 (2) (2004) 137–165. Available from: <https://doi.org/10.1177/0892705704035411>.
- [71] K.A. Fetfatsidis, L.M. Gamache, J.L. Gorczyca, J.A. Sherwood, D. Jauffrès, J. Chen, Design of an apparatus for measuring tool/fabric and fabric/fabric friction of woven-fabric composites during the thermostamping process, *Int. J. Material Form.* 6 (1) (2013) 1–11. Available from: <https://doi.org/10.1007/s12289-011-1058-3>.
- [72] R. Akkerman, R. ten Thije, U. Sachs, M. de Rooij, Friction in textile thermoplastic composites forming, in: C. Binetruy, F. Boussu (Eds.), *Proceedings of the 10th International Conference on Textile Composites - TEXCOMP 10: Recent Advances in Textile Composites*, 2010, pp. 271–279. January.
- [73] A.M. Murtagh, J.J. Lennon, P.J. Mallon, Surface friction effects related to pressforming of continuous fibre thermoplastic composites, *Compos. Manuf.* 6 (3–4) (1995) 169–175. [https://doi.org/10.1016/0956-7143\(95\)95008-M](https://doi.org/10.1016/0956-7143(95)95008-M). Available from: .
- [74] R.H.W. ten Thije, R. Akkerman, M. Ubbink, L. van der Meer, A lubrication approach to friction in thermoplastic composites forming processes, *Compos. Appl. Sci. Manuf.* 42 (8) (2011) 950–960. Available from: <https://doi.org/10.1016/j.compositesa.2011.03.023>.
- [75] I.M. Hutchings, *Tribology: Friction and Wear of Engineering Materials*, E. Arnold, 1992.
- [76] J.L. Gorczyca-Cole, J.A. Sherwood, J. Chen, A friction model for thermoforming commingled glass-polypropylene woven fabrics, *Compos. Appl. Sci. Manuf.* 38 (2) (2007) 393–406. Available from: <https://doi.org/10.1016/j.compositesa.2006.03.006>.
- [77] J.L. Gorczyca, J.A. Sherwood, L. Liu, J. Chen, Modeling of friction and shear in thermostamping of composites - Part I, *J. Compos. Mater.* 38 (21) (2004) 1911–1929. Available from: <https://doi.org/10.1177/0021998304048416>.
- [78] S. Liu, J. Sinke, C. Dransfeld, An inter-ply friction model for thermoset based fibre metal laminate in a hot-pressing process, *Compos. B Eng.* 227 (2021) 109400. Available from: <https://doi.org/10.1016/j.compositesb.2021.109400>.
- [79] J.M. Lee, B.M. Kim, C.J. Lee, D.C. Ko, A characterisation of tool-ply friction behaviors in thermoplastic composite, *Procedia Eng.* 207 (2017) 90–94. Available from: <https://doi.org/10.1016/j.proeng.2017.10.743>.
- [80] U. Sachs, R. Akkerman, S.P. Haanappel, R.H.W. ten Thije, M.B. de Rooij, Friction in forming of UD composites, *AIP Conf. Proc.* 1353 (April 2011) (2011) 984–989. Available from: <https://doi.org/10.1063/1.3589644>.
- [81] U. Sachs, R. Akkerman, K. Fetfatsidis, E. Vidal-Sallé, J. Schumacher, G. Ziegmann, et al., Characterization of the dynamic friction of woven fabrics: experimental methods and benchmark results, *Compos. Appl. Sci. Manuf.* 67 (2014) 289–298. Available from: <https://doi.org/10.1016/j.compositesa.2014.08.026>.
- [82] P. Harrison, R.T. Thije, R. Akkerman, A.C. Long, Characterising and modelling tool-ply friction of viscous textile composites, *World J. Eng.* 7 (1) (2010) 5–22. Available from: <http://eprints.gla.ac.uk/58158/>.
- [83] R. Scherer, K. Friedrich, Experimental background for finite element analysis of the interply-slip process during thermoforming of thermoplastic composites, *Dev. Sci. Technol. Comp. Mater.* (1990) 1001–1006. Available from: https://doi.org/10.1007/978-94-009-0787-4_144.
- [84] S. Chow, Frictional Interaction between Blank Holder and Fabric in Stamping of Woven Thermoplastic Composites, 2002.
- [85] R. Akkerman, M.P. Ubbink, M.B. de Rooij, R.H.W. ten Thije, Tool-ply friction in thermoplastic composite forming, *Int. J. Material Form.* 1 (SUPPL. 1) (2007) 953–956.
- [86] T.K. Slange, L.L. Warnet, W.J.B. Grouve, R. Akkerman, Deconsolidation of C/PEEK blanks: on the role of prepreg, blank manufacturing method and conditioning, *Compos. Appl. Sci. Manuf.* 113 (July) (2018) 189–199. Available from: <https://doi.org/10.1016/j.compositesa.2018.06.034>.
- [87] T.K. Slange, W.J.B. Grouve, L.L. Warnet, S. Wijskamp, R. Akkerman, Towards the combination of automated lay-up and stamp forming for consolidation of tailored composite components, *Compos. Appl. Sci. Manuf.* 119 (2019) 165–175. Available from: <https://doi.org/10.1016/j.compositesa.2019.01.016>.
- [88] A.C. Loos, P.H. Dara, Processing of thermoplastic matrix composites, in: D.O. Thompson, D.E. Chimenti (Eds.), *Review of Progress in Quantitative Nondestructive Evaluation*, Springer, Boston, MA, 1987, pp. 1257–1265. Available from: https://doi.org/10.1007/978-1-4613-1893-4_143.
- [89] T. Gereke, O. Döbrich, M. Hübner, C. Cherif, Experimental and computational composite textile reinforcement forming: a review, *Compos. Appl. Sci. Manuf.* 46 (1) (2013) 1–10. Available from: <https://doi.org/10.1016/j.compositesa.2012.10.004>.
- [90] P. Boisse, J. Colmars, N. Hamila, N. Naouar, Q. Steer, Bending and wrinkling of composite fiber preforms and prepregs. A review and new developments in the draping simulations, *Compos. B Eng.* 141 (2018) 234–249. Available from: <https://doi.org/10.1016/j.compositesb.2017.12.061>.
- [91] S.P. Haanappel, Forming of UD Fibre Reinforced Thermoplastics, PhD Thesis, 2013.
- [92] T.A. Martin, D. Bhattacharyya, R.B. Pipes, Deformation characteristics and formability of fibre-reinforced thermoplastic sheets, *Compos. Manuf.* 3 (3) (1992) 165–172. [https://doi.org/10.1016/0956-7143\(92\)90079-A](https://doi.org/10.1016/0956-7143(92)90079-A). Available from: .
- [93] B. Zouari, J.L. Daniel, P. Boisse, A woven reinforcement forming simulation method. Influence of the shear stiffness, *Comput. Struct.* 84 (5–6) (2006) 351–363. Available from: <https://doi.org/10.1016/j.compstruc.2005.09.031>.
- [94] P. Boisse, N. Hamila, A. Madeo, Modelling the development of defects during composite reinforcements and prepreg forming, *Phil. Trans. Math. Phys. Eng. Sci.* 374 (2071) (2016) 1–14. Available from: <https://doi.org/10.1098/rsta.2015.0269>.
- [95] B. Liang, N. Hamila, M. Peillon, P. Boisse, Analysis of the thermoplastic prepreg bending stiffness during manufacturing and of its influence on wrinkling simulations, *Compos. Appl. Sci. Manuf.* 67 (2014) 111–122. Available from: <https://doi.org/10.1016/j.compositesa.2014.08.020>.
- [96] R. Akkerman, S.P. Haanappel, Thermoplastic composites manufacturing by thermoforming [Internet], in: P. Boisse (Ed.), *Advances in Composites Manufacturing and Process Design*, Elsevier, 2015, pp. 111–129. Available from: <https://doi.org/10.1016/B978-1-78242-307-2.00006-3>.
- [97] X. Liu, F. Chen, A review of void formation and its effects on the mechanical performance of carbon fiber reinforced plastic, *Eng. Trans.* 64 (1) (2016) 33–51.
- [98] L. Ye, Z.R. Chen, M. Lu, M. Hou, De-consolidation and re-consolidation in CF/PPS thermoplastic matrix composites, *Compos. Appl. Sci. Manuf.* 36 (7) (2005) 915–922. Available from: <https://doi.org/10.1016/j.compositesa.2004.12.006>.
- [99] B. Zheng, M. Li, T. Deng, H. Zhou, Z. Huang, H. Zhou, et al., Process-structure-property relationships of thermoformed woven carbon-fiber-reinforced polyether-ether-ketone composites, *Polym. Compos.* 40 (10) (2019) 3823–3834. Available from: <https://doi.org/10.1002/pc.25241>.
- [100] D. Trudel-Boucher, B. Fisa, J. Denault, P. Gagnon, Experimental investigation of stamp forming of unconsolidated commingled E-glass/polypropylene fabrics, *Compos. Sci. Technol.* 66 (3–4) (2006) 555–570. Available from: <https://doi.org/10.1016/j.compscitech.2005.05.036>.
- [101] A. Beehag, L. Ye, Role of cooling pressure on interlaminar fracture properties of commingled CF/PEEK composites, *Compos. Appl. Sci. Manuf.* 27 (3 PART A) (1996) 175–182. [https://doi.org/10.1016/1359-835X\(95\)00027-Y](https://doi.org/10.1016/1359-835X(95)00027-Y). Available from: .
- [102] W. Jiang, Z. Huang, Y. Wang, B. Zheng, H. Zhou, Voids formation and their effects on mechanical properties in thermoformed carbon fiber fabric-reinforced composites, *Polym. Compos.* 40 (S2) (2019) E1094–E1102. Available from: <https://doi.org/10.1002/pc.24876>.
- [103] G. Dai, L. Zhan, C. Guan, M. Huang, The effect of moulding process parameters on interlaminar properties of CF/PEEK composite laminates, *High Perform. Polym.* 32 (7) (2020) 835–841. Available from: <https://doi.org/10.1177/F0954008320903768>.
- [104] P.Y.B. Jar, R. Mulone, P. Davies, H.H. Kausch, A study of the effect of forming temperature on the mechanical behaviour of carbon-fibre/peek composites, *Compos. Sci. Technol.* 46 (1) (1993) 7–19. [https://doi.org/10.1016/0266-3538\(93\)90076-S](https://doi.org/10.1016/0266-3538(93)90076-S). Available from: .
- [105] T. Vu-Khanh, J. Denault, Effect of molding parameters on the interfacial strength in PEEK/carbon composites, *J. Reinforc. Plast. Compos.* 12 (8) (1993) 916–931. Available from: <https://doi.org/10.1177/073168449301200806>.
- [106] N. Reynolds, S. Awang-Ngah, G. Williams, D.J. Hughes, Direct processing of structural thermoplastic composites using rapid isothermal stamp forming, *Appl. Compos. Mater.* 27 (1–2) (2020) 107–115. Available from: <https://doi.org/10.1007/s10443-020-09797-4>.
- [107] P. Patel, T.R. Hull, R.W. McCabe, D. Flath, J. Grasmeder, M. Percy, Mechanism of thermal decomposition of poly(ether ether ketone) (PEEK) from a review of decomposition studies, *Polym. Degrad. Stab.* 95 (5) (2010) 709–718. Available from: <https://doi.org/10.1016/j.polydegradstab.2010.01.024>.
- [108] L. Sang, C. Wang, Y. Wang, Z. Wei, Thermo-oxidative ageing effect on mechanical properties and morphology of short fibre reinforced polyamide composites-comparison of carbon and glass fibres, *RSC Adv.* 7 (69) (2017) 43334–43344. Available from: <https://doi.org/10.1039/C7RA07884F>.

- [109] S. Rathi, J.B. Dahiya, Effect on thermal behaviour of polyamide 66/clay nanocomposites with inorganic flame retardant additives, *Indian J. Chem. - Section A Inorganic Phys. Theor. Analyt. Chem.* 51 (12) (2012) 1677–1685. Available from: <http://nopr.niscair.res.in/handle/123456789/15206>.
- [110] G. Montaudo, C. Puglisi, F. Samperi, Primary thermal degradation processes occurring in poly(phenylenesulfide) investigated by direct pyrolysis–mass spectrometry, *J. Polym. Sci. Polym. Chem.* 32 (10) (1994) 1807–1815. Available from: <https://doi.org/10.1002/pola.1994.080321002>.
- [111] M. Hou, K. Friedrich, R. Scherer, Optimization of stamp forming of thermoplastic composite bends, *Compos. Struct.* 27 (1–2) (1994) 157–167. Available from: [https://doi.org/10.1016/0263-8223\(94\)90077-9](https://doi.org/10.1016/0263-8223(94)90077-9).
- [112] P. Land, R. Crossley, D. Branson, S. Ratchev, Technology review of thermal forming techniques for use in composite component manufacture, *SAE Int. J. Mater. Manufact.* 9 (1) (2016) 81–89. Available from: <https://doi.org/10.4271/2015-01-2610>.
- [113] J. Chen, J.A. Sherwood, P. Buso, S. Chow, D. Lussier, Stamping of continuous fiber thermoplastic composites, *Polym. Compos.* 21 (4) (2000) 539–547. Available from: <https://doi.org/10.1002/pc.10209>.
- [114] M. Hou, K. Friedrich, 3-D stamp forming of thermoplastic matrix composites, *Appl. Compos. Mater.* 1 (2) (1994) 135–153. Available from: <https://doi.org/10.1007/BF00567575>.
- [115] B. Vieille, W. Albouy, L. Taleb, Investigations on stamping of C/PEEK laminates: influence on meso-structure and macroscopic mechanical properties under severe environmental conditions, *Compos. B Eng.* 63 (2014) 101–110. Available from: <https://doi.org/10.1016/j.compositesb.2014.03.025>.
- [116] S.L. Gao, J.K. Kim, Cooling rate influences in carbon fibre/PEEK composites. Part I. Crystallinity and interface adhesion, *Compos. Appl. Sci. Manuf.* 31 (6) (2000) 517–530. Available from: [https://doi.org/10.1016/S1359-835X\(00\)00009-9](https://doi.org/10.1016/S1359-835X(00)00009-9).
- [117] S.L. Gao, J.K. Kim, Correlation among crystalline morphology of PEEK, interface bond strength, and in-plane mechanical properties of carbon/PEEK composites, *J. Appl. Polym. Sci.* 84 (6) (2002) 1155–1167. Available from: <https://doi.org/10.1002/app.10406>.
- [118] D. Tatsuno, T. Yoneyama, K. Kawamoto, M. Okamoto, Effect of cooling rate on the mechanical strength of carbon fiber-reinforced thermoplastic sheets in press forming, *J. Mater. Eng. Perform.* 26 (7) (2017) 3482–3488. Available from: <https://doi.org/10.1007/s11665-017-2664-0>.
- [119] J. Weber, J. Schlimbach, Co-consolidation of CF/PEEK tape-preforms and CF/PEEK organo sheets to manufacture reinforcements in stamp-forming process, *Adv. Manuf. Polym. Compos. Sci.* 5 (4) (2019) 172–183. Available from: <https://doi.org/10.1080/20550340.2019.1673961>.
- [120] S.-L. Gao, J.-K. Kim, Cooling rate influences in carbon fibre/PEEK composites. Part II: interlaminar fracture toughness, *Compos. Appl. Sci. Manuf.* 32 (6) (2001) 763–774. Available from: [https://doi.org/10.1016/S1359-835X\(00\)00188-3](https://doi.org/10.1016/S1359-835X(00)00188-3).
- [121] P.P. Parlevliet, H.E.N. Bersee, A. Beukers, Residual stresses in thermoplastic composites-A study of the literature-Part I: formation of residual stresses, *Compos. Appl. Sci. Manuf.* 37 (11) (2006) 1847–1857. Available from: <https://doi.org/10.1016/j.compositesa.2005.12.025>.